Chromatin Conformation Links Putative Enhancers in Intracranial Aneurysm–Associated Regions to Potential Candidate Genes

Melanie D. Laarman, MSc; Geert Geeven, PhD; Phil Barnett, PhD; Netherlands Brain Bank; Gabriël J. E. Rinkel, MD, PhD; Wouter de Laat, PhD; Ynte M. Ruigrok, MD, PhD*; Jeroen Bakkers, PhD*

Background—We previously showed that intracranial aneurysm (IA)–associated single-nucleotide polymorphisms are enriched in promoters and putative enhancers identified in the human circle of Willis, on which IAs develop, suggesting a role for promoters and enhancers in IAs. We further investigated the role of putative enhancers in the pathogenesis of IA by identifying their potential target genes and validating their regulatory activity.

Methods and Results—Using our previously published circle of Willis chromatin immunoprecipitation and sequencing data, we selected 34 putative enhancers in IA-associated regions from genome-wide association studies. We then used a chromatin conformation capture technique to prioritize target genes and found that 15 putative enhancers interact with the promoters of 6 target genes: *SOX17*, *CDKN2B*, *MTAP*, *CNNM2*, *RPEL1*, and *GATA6*. Subsequently, we assessed the activity of these putative enhancers in vivo in zebrafish embryos and confirmed activity for 8 putative enhancers. Last, we found that all 6 target genes are expressed in the circle of Willis, on the basis of RNA sequencing data and in situ hybridization. Furthermore, in situ hybridization showed that these genes are expressed in multiple cell types in the circle of Willis.

Conclusions—In 4 of 6 IA-associated genome-wide association study regions, we identified 8 putative enhancers that are active in vivo and interact with 6 nearby genes, suggesting that these genes are regulated by the identified putative enhancers. These genes, *SOX17*, *CDKN2B*, *MTAP*, *CNNM2*, *RPEL1*, and *GATA6*, are therefore potential candidate genes involved in IA pathogenesis and should be studied using animal models in the future. (*J Am Heart Assoc*. 2019;8:e011201. DOI: 10.1161/JAHA.118. 011201.)

Key Words: circle of Willis • gene regulation • intracranial aneurysm • single-nucleotide polymorphism • zebrafish

Rupture of an intracranial aneurysm (IA) results in an aneurysmal subarachnoid hemorrhage. The consequences of an aneurysmal subarachnoid hemorrhage are enormous because of the relatively young age at which it occurs (mean age, 50 years) and the high case fatality and morbidity.[1]

Genome-wide association studies (GWASs) have identified single-nucleotide polymorphisms (SNPs) associated with IA that are located within 6 genomic risk loci (4q31.23, 8q11.23–q12.1, 9p21.3, 10q24.32, 13q13.1, and 18q11.2).[2–4] These SNPs may not be causal, but rather may be in linkage disequilibrium with the causal variants. Therefore, the entire genomic regions spanning the SNPs in strong linkage disequilibrium with the IA-associated SNPs should be investigated in search of the causal variants.

We recently showed that IA-associated SNPs are enriched in promoters and putative enhancers of the human circle of Willis (CoW), on which IAs develop, suggesting a role for such regulatory regions in IAs.[5] In this study, we further investigated the role of these putative enhancers in the pathogenesis of IA by identifying their potential target genes and validating their regulatory activity. Specifically, we first aimed to select those putative enhancers that physically interact with the promoter of a nearby gene, thereby also identifying

---

<div style="border: 2px solid red; padding: 10px;">

Clinical Perspective

What Is New?

- Enhancers in intracranial aneurysm–associated regions from genome-wide association studies interact with promoters in proximity, and most of these enhancers are active in a zebrafish reporter assay.
- The genes that these enhancers interact with are expressed in the circle of Willis.
- These genes are potential candidates to study intracranial aneurysm pathogenesis.

What Are the Clinical Implications?

- Further studying the identified potential candidate genes will reveal new insights into intracranial aneurysm pathogenesis.
- This may lead to the development of new therapies that prevent aneurysm development or inhibit growth or rupture.

</div>

the potential target genes of these putative enhancers, using chromatin conformation capture technology (4C; a screening method for DNA interaction) on human CoW specimens. Next, we aimed at assessing the intrinsic enhancer activity of these putative enhancers in vivo in zebrafish embryos, followed by gene expression analysis of the identified target genes.

Methods

The data sets discussed in this publication have been made publicly available in the National Center for Biotechnology Information Gene Expression Omnibus database and can be accessed through Gene Expression Omnibus Series accession number GSE115304.

Human Material

Four CoW specimens were obtained from the Netherlands Brain Bank, Netherlands Institute for Neuroscience, Amsterdam. All material was collected from donors whose written informed consent for brain autopsy and the use of the material and clinical information for research purposes had been obtained by the Netherlands Brain Bank (http://www.brainbank.nl). Approval for the study was obtained from the institutional review board of the Netherlands Brain Bank. Donor and sample characteristics can be found in Table S1.

The 4 CoW specimens were used for 3 different experiments (Table S1). Two CoW specimens (CoW1 and CoW2) were flash frozen in liquid nitrogen and stored at −80°C until further use for the 4C experiments. The third CoW specimen (CoW3) was also flash frozen in liquid nitrogen, after which RNA was isolated and used to generate cDNA for in situ

hybridization (ISH) antisense probe synthesis. The fourth CoW specimen (CoW4) was fixed in 4% paraformaldehyde for 20 hours, washed in PBS twice, dehydrated in ethanol, embedded in paraffin, and divided into 4-μm–thick sections for ISH.

We used DNA from Dutch participants in the GWAS on IA[2–4] to amplify putative enhancer sequences for in vivo enhancer activity testing,

Selection of Putative Enhancers and Their Potential Target Genes on the Basis of Physical Contact

For the purpose of this study, we selected all putative enhancers within the 6 GWAS-identified regions most strongly associated with IA: 4q31.23, 8q11.23-12.1, 9p21.3, 10q24.32, 13q13.1, and 18q11.2.[2–4] These regions were defined as the entire genomic region spanning the SNPs in strong linkage disequilibrium ($r^2 \geq 0.8$, using HaploReg,[6] on the basis of the 1000 Genomes Project) with the IA-associated SNPs (genomic regions in Table 1).

Within these IA-associated regions, putative enhancers to use for 4C were selected on the basis of H3K27ac enrichment in our previously published chromatin immunoprecipitation and sequencing (ChIP-seq) data,[5] using the peak calling algorithms MACS2 (enhancer peaks from Laarman et al[5]) and OccuPeak (using $P=10^{-12}$).[7] Because putative enhancers did not need to directly overlap with an IA-associated SNPs to be selected for the current study, this approach resulted in more putative enhancers than in our previous study.[5] In addition, we also added putative enhancers to the selection if we observed an enrichment of reads in 4C experiments for other putative enhancers or promoters in this study. These putative enhancers were not in the initial selection because the H3K27ac ChIP-seq enrichment was not called by one of the peak calling algorithms. On the basis of the 4C experiments, however, there was contact with other putative enhancers or a promoter, suggestive of interaction. Therefore, these putative enhancers were added to the selection.

Table 1. Coordinates of IA-Associated Regions

Locus	Genomic Coordinates of IA-Associated Regions
4q31.23	Chromosome 4: 148364920-148414652
8q11.23-q12.1	Chromosome 8: 55288149-55328345
	Chromosome 8: 55407312-55462325
9p21.3	Chromosome 9: 22072264-22125504
10q24.32	Chromosome 10: 104638480-104958901
13q13.1	Chromosome 13: 33672530-33725688
18q11.2	Chromosome 18: 20145379-20280647

IA indicates intracranial aneurysm.

To measure contact frequencies between our selected set of putative enhancers and promoters of nearby candidate target genes, we used 4C (Figure 1A). In short, bait fragments, or baits, from where chromatin interactions with other DNA regions are investigated, were designed for all putative enhancers to identify interacting DNA fragments for each putative enhancer. Subsequently, baits were designed for candidate target promoters for which the 4C results from the putative enhancers suggested there was physical contact with at least one of the selected putative enhancers (primers in Table S2). We used 2 CoWs (Table S1) for 4C.

The 4C experiments were conducted as described previously.[8,9] Frozen (−80°C) CoW tissue was homogenized by disrupting it using a Mixer Mill MM 400 tissue disrupter (Retsch GmbH) twice at 30 Hz for 45 seconds, with refreezing in liquid nitrogen in between. Tissue powder was cross-linked and further processed, as described previously,[8,9] using DpnII and Csp6I as restriction enzymes. The primers used for amplification of the genomic regions (bait fragments) used to search for interaction partners of the selected enhancers can be found in Table S2. Amplified fragments were sequenced on the Illumina HiSeq2000 or the Illumina NextSeq500 genome sequencer. Sequence reads were mapped to the human genome (hg19). Reads mapping to multiple fragment ends were removed. 4C coverage was computed by averaging mapped reads in running windows of 21 fragment ends. Quality assessment was done, as previously described.[8] Only data sets that showed a *cis/* total ratio of mapped 4C captures of at least 40%, and 4C fragment end coverage in a 200 kilobase (kb) window around the viewpoint of at least 35% were included in the analysis (quality assessments of 4C data sets in Table S3).

On the basis of visual inspection of the results from the 4C experiments in a genome browser, we selected those putative enhancers that showed localized increased 4C contact frequencies with potential target promoters suggestive of 3-dimensional spatial interaction.

Assessment of Enhancer Activity

The intrinsic activity of the putative enhancers thus selected using 4C was tested using an enhancer reporter assay in zebrafish embryos. Putative enhancers were amplified using DNA of participants in the IA GWAS[2–4] that carried the reference allele in the locus of the amplified putative enhancer. Consequently, we tested the activity of the reference sequences. Primers used for amplification are described in Table S4. The amplified putative enhancers were cloned into an enhancer reporter vector containing the E1b minimal promoter, followed by the green fluorescent protein (GFP) gene (E1b-GFP-Tol2-Gateway; Addgene plasmid No. 37846),[10] using Gateway technology (Life Technologies BV).

The resulting reporter constructs were injected in the cell of wild-type zebrafish embryos at the 1-cell stage, at a final concentration of 10 ng/μL plasmid and 25 ng/μL TOL2 transposase RNA (for incorporation into the zebrafish genome). Embryos were kept at 28.5°C, and GFP expression was assessed between 2 and 5 days after fertilization using a Leica M165 FC fluorescent stereomicroscope (Leica Microsystems GmbH).

Expression of Target Genes

To analyze the expression of the potential target genes identified with 4C, we first investigated whether these genes are expressed in the CoW using our previously published RNA sequencing data.[5] We subsequently performed ISH on 4-μm CoW paraffin sections to determine the expression patterns within the CoW vessel wall. Antisense RNA probes were designed against the human cDNA sequence of the target genes and selected control genes for 3 different cell types in the CoW: endothelial cells (*EDN1* and *VWF*), vascular smooth muscle cells (VSMCs; *ACTA2* and *TAGLN*), and fibroblasts (*FN1*). The primers used to generate these probes are described in Table S5. RNA from CoW3 (Table S1) was used to generate cDNA for probe synthesis. ISH was performed as described previously.[11]

Results

Selection of Putative Enhancers and Their Potential Target Genes on the Basis of Physical Contact

We selected 30 putative enhancers within the genomic regions spanning the SNPs in strong linkage disequilibrium with the IA-associated SNPs (hereafter referred to as IA-associated regions; Table 1), on the basis of our previously published ChIP-seq data.[5] Four putative enhancers were added to the selection on the basis of an enrichment of reads in 4C experiments using other putative enhancers or promoters as baits: the enhancers with bait numbers 13, 14, and 17 were added on the basis of an enrichment of reads in the 4C from promoters *CDKN2B* (baits 13, 14, and 17) and *MTAP* (only bait 17; Table S2 and Figure S1), and the enhancer with bait number 44 was added on the basis of an enrichment of reads in the 4C experiment from the enhancers with bait numbers 39, 42, 43, and 45 (Table S2 and Figure S1). This resulted in a total of 34 selected putative enhancers to be used in the 4C experiments (Table S2). Table S2 also describes the basis on which each putative enhancer was selected: it shows with which peak calling algorithm the enrichment of ChIP-seq reads was identified or if the putative enhancer was identified on the
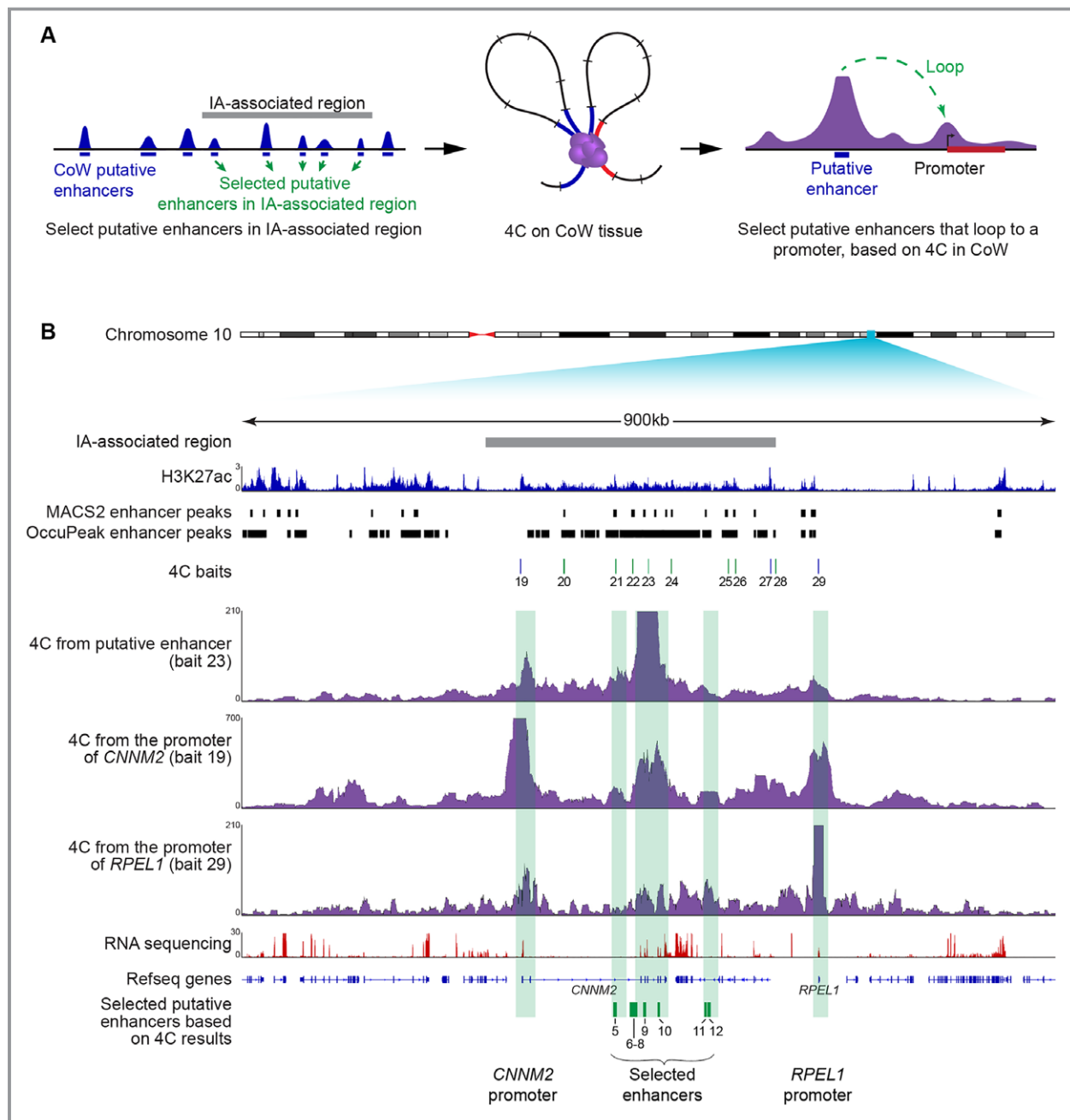
Figure 1. Chromatin conformation capture technology (4C) identifies physical interaction between putative enhancers in intracranial aneurysm (IA)–associated regions and nearby promoters. **A**, Graphical representation of the experimental setup. Putative enhancers were selected within IA-associated regions, on the basis of our previously published chromatin immunoprecipitation and sequencing (ChIP-seq) data in the circle of Willis (CoW).[5] 4C experiments were performed for the selected putative enhancers to identify physical interactions between these putative enhancers and nearby promoters. **B**, Genome browser view of a 900 kilobase example region, on chromosome 10, that contains an IA-associated region. This graph shows our previously published ChIP-seq data[5] for histone modification H3K27ac, including the enhancer peaks identified using peak calling algorithms MACS2[5] and OccuPeak,[7] the baits used for 4C (promoters in blue, putative enhancers in green), the results of 3 4C experiments (1 in which a selected putative enhancer was used as the bait, and 2 in which a promoter was used as the bait [*CNNM2* and *RPEL1*]), and our previously published RNA-seq (RNA sequencing) data.[5] Within this locus, 8 putative enhancers were selected for which an interaction with a promoter of a gene expressed in the CoW was observed. **C**, Overview of the 6 IA-associated regions, the number of baits used for 4C (including both putative enhancers and promoters), the genes for which an interaction was observed between the promoter and a putative enhancer, and the number of putative enhancers selected for further investigation.

	IA-associated region on chromosome	No. of 4C baits	Loops between putative enhancers and promoters of genes	No. of selected putative enhancers
C	4	5	-	0
	8	5	*SOX17*	1
	9	8	*MTAP, CDKN2B*	3
	10	11	*CNNM2, RPEL1*	8
	13	6	-	0
	18	11	*GATA6*	3

Figure 1. Continued

basis of enrichment of reads in another 4C experiment in this study.

To systematically study 3-dimensional spatial contacts and identify potential functionally important links between our selected set of putative enhancers located in IA-associated regions and their target genes, we implemented the following 4C strategy. We designed baits for both the 34 selected putative enhancers and a set of 12 promoters for which the 4C results from the putative enhancers suggested there was physical contact with at least one of the selected putative enhancers (basis for selection of each promoter in Table S2). Of these 46 4C experiments, 40 were successful and met our quality criteria (29 putative enhancers and 11 promoters; Figure S2 and Table S3). The experiments for 7 baits were performed in 2 CoW samples, and the results from these replicated experiments were comparable (panels for the replicated experiments are incorporated in Figures S3 through S6).

On the basis of visual inspection for increased contact frequencies in the 4C results, we found evidence of physical contact between 12 putative enhancers and the promoters of 6 genes: *SOX17* (8q11.23-q12.1), *CDKN2B* (9p21.3), *MTAP* (9p21.3), *CNNM2* (10q24.32), *RPEL1* (10q24.32), and *GATA6* (18q11.2) (Figure 1B and 1C; Table 2). Most of these interactions were reciprocally confirmed by looking both from the enhancer and from the gene promoter (Table S6). We did not find convincing evidence of physical interaction between the putative enhancers in the IA-associated regions on chromosomes 4 and 13 and the promoters of any nearby genes. Therefore, these putative enhancers were not investigated further.

Visual representations of the 4C results and the selected putative enhancers in all 6 IA-associated regions are shown in Figures 2 through 7.

Together, these results indicate that 12 of 34 putative enhancers show an increased contact frequency with nearby

Table 2. Summary of 4C, ISH, and Enhancer Activity

IA-Associated Region	Putative Enhancer Baits	Interaction With Promoter of Genes	Expression in the CoW on the Basis of ISH	Selected Putative Enhancers That Interact With Promoter	Intrinsically Active Putative Enhancers
Chromosome 4: 148364920-148414652	3	–	–	–	–
Chromosome 8: 55288149-55328345	4	*SOX17*	Intima, media, and adventitia	1	1
Chromosome 8: 55407312-55462325	0	–	–	–	–
Chromosome 9: 22072264-22125504	6	*MTAP* and *CDKN2B*	Intima and media for *MTAP*, *CDKN2B* not tested because of technical failure	3	1
Chromosome 10: 104638480-104958901	9	*CNNM2* and *RPEL1*	Intima, media, and adventitia for both genes	8 for *CNNM2*, 7 for *RPEL1*	5 (2 not tested because of technical failure)
Chromosome 13: 33672530-33725688	4	–	–	–	–
Chromosome 18: 20145379-20280647	8	*GATA6*	Intima and media	3	1 (2 not tested because of technical failure)

4C indicates chromatin conformation capture technology; CoW, circle of Willis; IA, intracranial aneurysm; ISH, in situ hybridization.
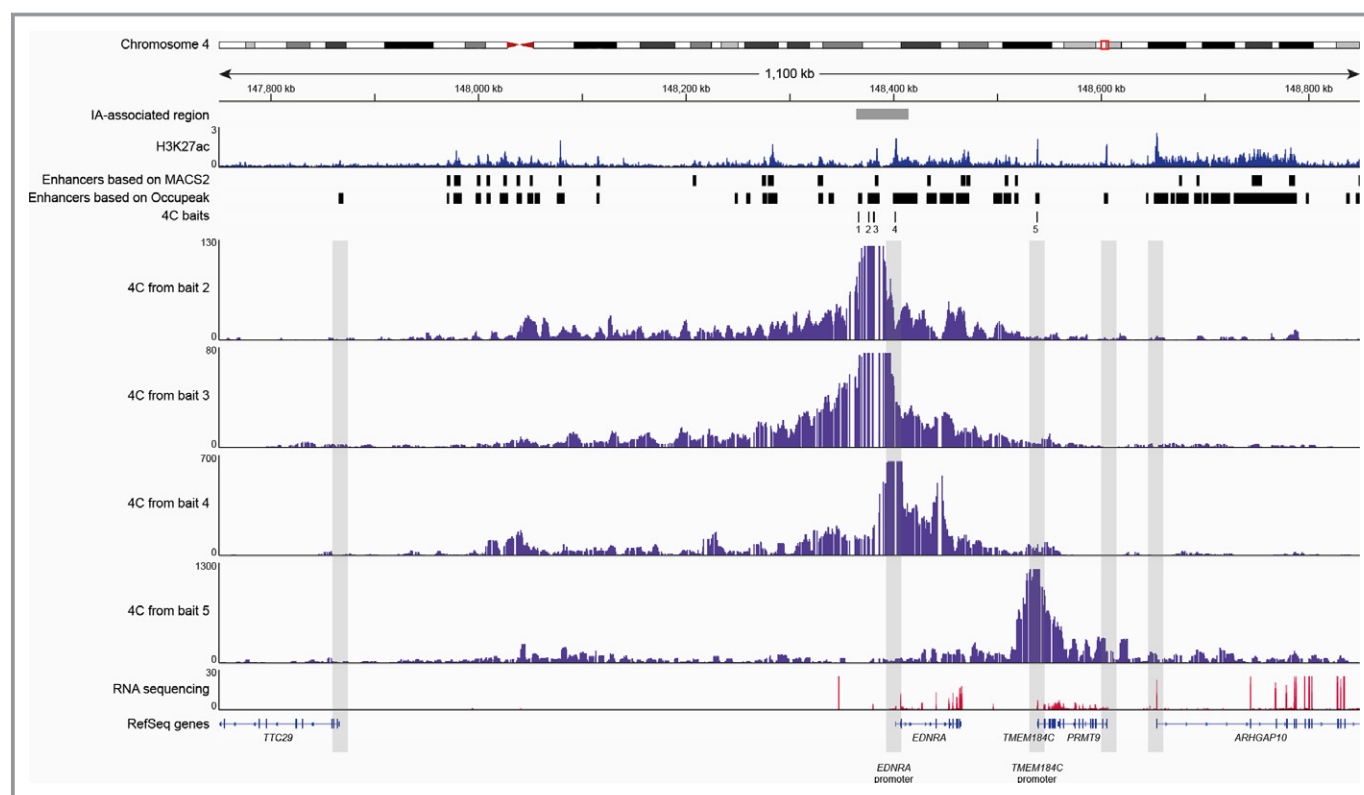
Figure 2. Chromosomal interactions around the intracranial aneurysm (IA)–associated region on chromosome 4. Genome browser view of an 1100 kilobase example region on chromosome 4, which contains an IA-associated region. This graph shows a combination of multiple types of data. First, the localization of the IA-associated regions on the chromosome is shown. Then, our previously published chromatin immunoprecipitation and sequencing data for histone modification H3K27ac are shown,[5] including the enhancer peaks called using peak calling algorithms MACS2[5] and OccuPeak.[7] Next, the chromatin conformation capture technology (4C) baits that were selected by combining the results of the 2 peak calling algorithms are shown. Then, the 4C results from this region are shown for those of the 5 baits that were chosen for which the 4C experiment was successful. Baits 4 and 5 are promoters of the genes *EDNRA* and *TMEM184C*. Next, our previously published RNA sequencing data are shown.[5] No putative enhancers were selected in this region because there was no evidence of interactions between enhancers and promoters.

promoters in our 4C data, suggestive of 3-dimensional spatial interaction, and can therefore be prioritized as functional enhancers involved in regulating levels of transcription levels of the genes that they are in contact with: *SOX17*, *CDKN2B*, *MTAP*, *CNNM2*, *RPEL1*, and *GATA6*. These putative enhancers and genes were, therefore, selected for further investigation.

Assessment of Enhancer Activity

We used our previously published ChIP-seq data[5] and online available ENCODE (Encyclopedia of DNA Elements) data sets (H3K27ac ChIP-seq and transcription factor ChIP-seq) to determine the genomic coordinates of the 12 selected putative enhancers more precisely (coordinates in Table 3). For 2 of these putative enhancers, the CoW ChIP-seq H3K27ac enrichment was broad ($\approx$10 kb) and seemed to consist of multiple separate enrichment peaks. Therefore, these 2 putative enhancers were divided into multiple putative enhancers for enhancer activity assessment: one putative enhancer was divided into putative enhancers 6, 7, and 8

(Figure S7A), and the other enhancer was divided into putative enhancers 11 and 12 (Figure S7B). This resulted in a total of 15 putative enhancers for enhancer activity assessment (Table 3).

An initial search for available information on enhancer activity in the VISTA Enhancer Browser[12] showed that none of the enhancers on chromosomes 8, 10, and 18 were present in the database, and the 2 enhancers on chromosome 9 (enhancers 2 and 4) that were present in the database did not result in a detected reproducible activity at embryonic day 11.5 of mouse development. However, because this database only contains information for a single time point during mouse development, this does not mean that these enhancers are not active.[12]

We successfully cloned 11 of the 15 selected putative enhancers into the E1b enhancer reporter vector for further functional analysis in zebrafish embryos (Figure 8A). For the other 4 putative enhancers, the cloning did not work because of technical failure. Although injection of the empty control vector in zebrafish embryos did not result in any clear fluorescence, injection of 8 of the 11 enhancer vectors resulted in clear GFP
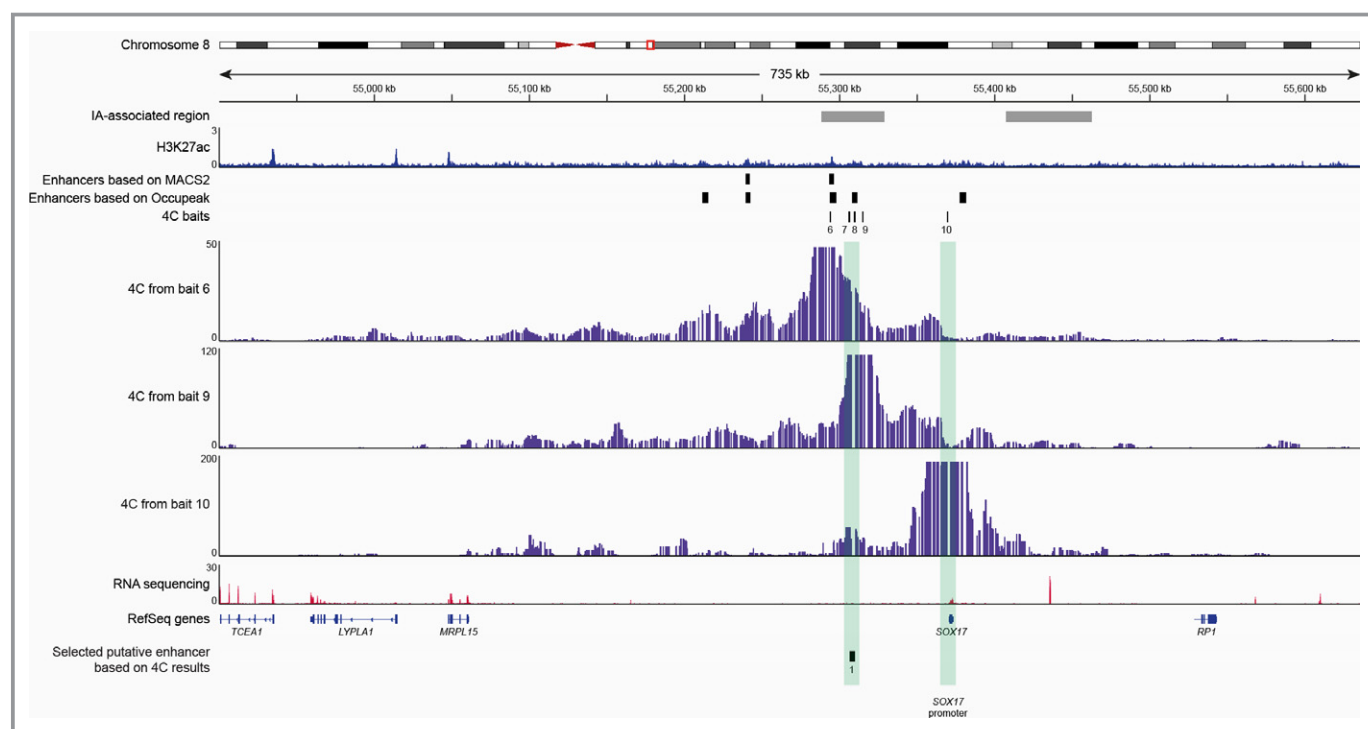
Figure 3. Chromosomal interactions around the intracranial aneurysm (IA)–associated region on chromosome 8. Genome browser view of a 735 kilobase example region on chromosome 8, which contains an IA-associated region. This graph shows a combination of multiple types of data. First, the localization of the IA-associated region on the chromosome is shown. Then, our previously published chromatin immunoprecipitation and sequencing data for histone modification H3K27ac are shown,[5] including the enhancer peaks called using peak calling algorithms MACS2[5] and OccuPeak.[7] Next, the chromatin conformation capture technology (4C) baits that were selected by combining the results of the 2 peak calling algorithms are shown. Then, the 4C results from this region are shown for those of the 5 baits that were chosen for which the 4C experiment was successful. Bait 10 is the promoter of the gene *SOX17*. Next, our previously published RNA sequencing data are shown.[5] Last, the graph shows the putative enhancer that was selected in this region because of its interaction with the promoter of *SOX17*.

expression in the embryo in the first 5 days after fertilization (Figure 8B and 8C; Figure S8; Table 2), suggesting that these putative enhancers are functional in vivo.

These results demonstrate that >70% of the putative enhancers that were selected on the basis of our criteria display enhancer activity in vivo.

Expression of Target Genes

To assess the expression of the identified potential candidate genes for IA, we first looked into our previously published CoW RNA sequencing data.[5] On the basis of these data, 5 of the 6 genes are expressed in the CoW. Expression of the sixth gene, *RPEL1*, was found in only 1 of the 4 CoWs; and this expression was low (Figure 9A).

To assess the expression pattern of the candidate genes in the vascular wall of the CoW, we compared the ISH-stained paraffin sections of the CoW (Figure 9A and 9B; Table 2) with those of selected control genes known to be expressed in endothelial cells (*VWF* and *EDN1*), VSMCs (*ACTA2* and *TAGLN*), and fibroblasts (*FN1*; Figure S9). Most of the CoW sections that were used contained a thickened intima

suggestive of atherosclerosis.[13] For 1 of the 6 candidate genes, *CDKN2B*, we were unable to generated a probe to assess the expression pattern because of technical failure.

The expression pattern of *SOX17* appeared similar to that of endothelial cell markers *VWF* and *EDN1*. There was staining for *SOX17* in all 3 layers of the CoW vascular wall, although only sparsely in the adventitia. The expression pattern of *MTAP* looked most similar to that of fibroblast marker *FN1*, but the staining for *MTAP* was weaker and there was no staining in the adventitia. The expression patterns of *CNNM2* and *RPEL1* were most similar to those of VSMC markers *ACTA2* and *TAGLN*, and some of the smaller stained foci looked similar to the staining of fibroblast marker *FN1*. The expression pattern of *GATA6* looked similar to the expression patterns of VSMC markers *ACTA2* and *TAGLN* and of fibroblast marker *FN1*. These results suggest that our IA candidate genes are expressed in all 3 major cell types of the vessel wall.

Discussion

We used 4C to identify the potential target genes for 8 intrinsically active putative enhancers, residing in 4 of the 6
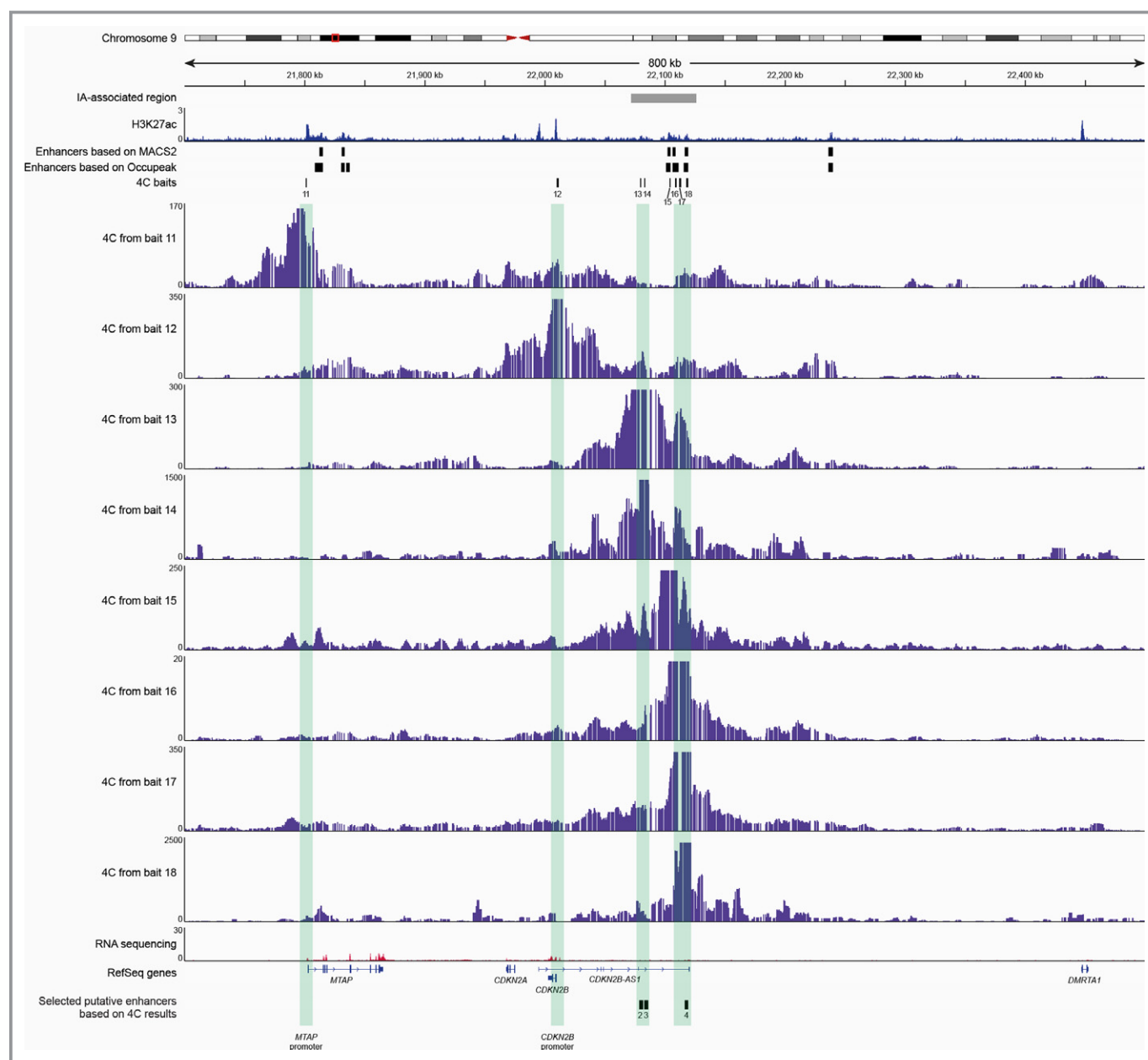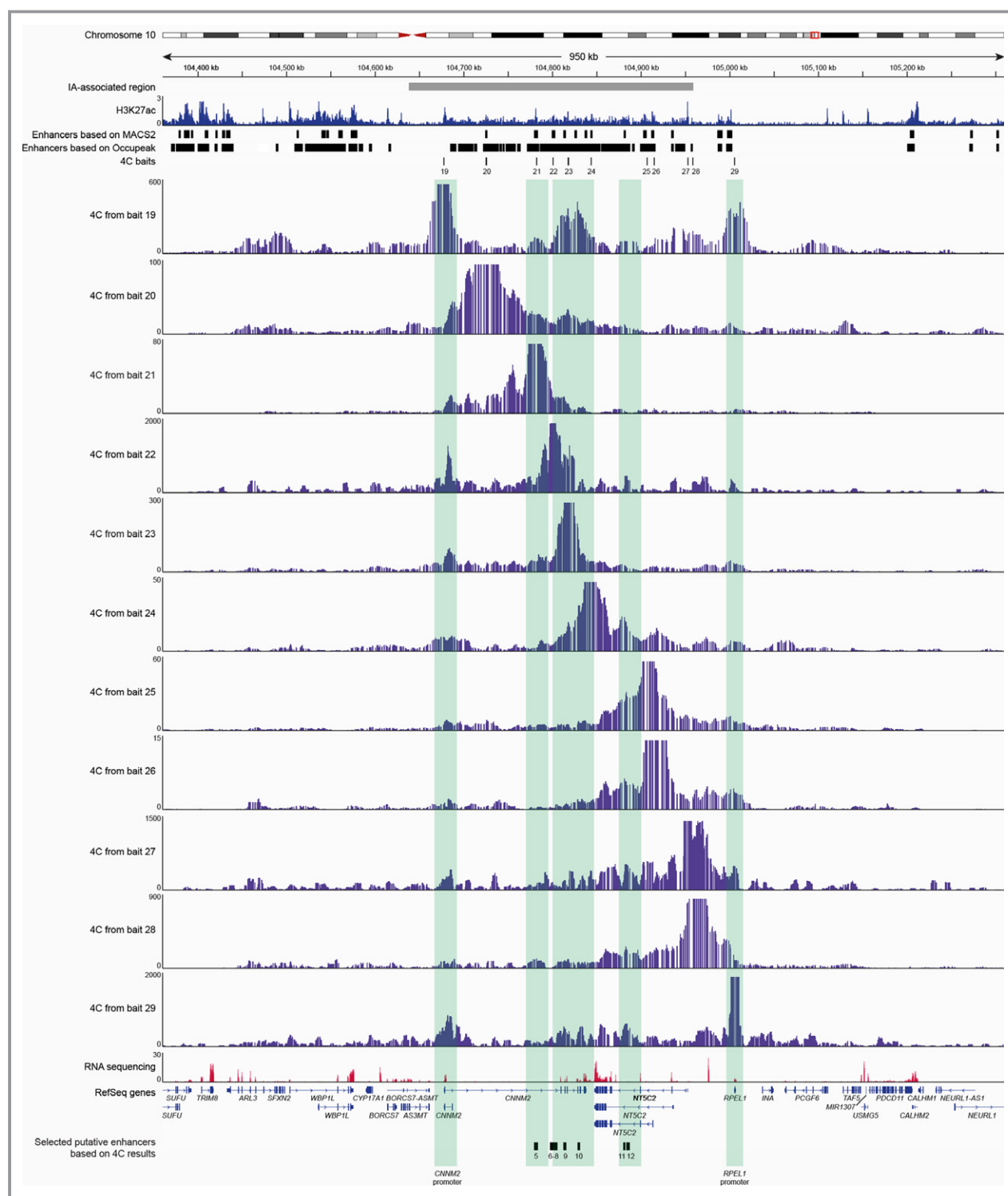
Figure 4. Chromosomal interactions around the intracranial aneurysm (IA)–associated region on chromosome 9. Genome browser view of an 800 kilobase example region on chromosome 9, which contains an IA-associated region. This graph shows a combination of multiple types of data. First, the localization of the IA-associated region on the chromosome is shown. Then, our previously published chromatin immunoprecipitation and sequencing data for histone modification H3K27ac are shown,[5] including the enhancer peaks called using peak calling algorithms MACS2[5] and OccuPeak.[7] Next, the chromatin conformation capture technology (4C) baits that were selected by combining the results of the 2 peak calling algorithms are shown. Then, the 4C results from this region for those of the 8 baits that were chosen for which the 4C experiment was successful are shown. Baits 11 and 12 are promoters of the genes *MTAP* and *CDKN2B*, respectively. Next, our previously published RNA sequencing data are shown.[5] Last, the graph shows the 3 putative enhancers that were selected in this region because of their interaction with the promoters of *MTAP* and *CDKN2B*.

known genomic risk loci associated with IA (being 4q31.23, 8q11.23–q12.1, 9p21.3, 10q24.32, 13q13.1, and 18q11.2). The likely target genes of these putative enhancers, *SOX17* (8q11.23–q12.1), *CDKN2B* (9p21.3), *MTAP* (9p21.3), *CNNM2* (10q24.32), *RPEL1* (10q24.32), and *GATA6* (18q11.2), are all

expressed in various cell types of the CoW and are, thus, potential candidate genes for IA pathogenesis.

In all IA-associated regions in which we investigated intrinsic enhancer activity, we found that at least one of the selected putative enhancers was capable of inducing GFP

Figure 5. Chromosomal interactions around the intracranial aneurysm (IA)–associated region on chromosome 10. Genome browser view of a 950 kilobase example region on chromosome 10, which contains an IA-associated region. This graph shows a combination of multiple types of data. First, the localization of the IA-associated region on the chromosome is shown. Then, our previously published chromatin immunoprecipitation and sequencing data for histone modification H3K27ac are shown,[5] including the enhancer peaks called using peak calling algorithms MACS2[5] and OccuPeak.[7] Next, the chromatin conformation capture technology (4C) baits that were selected by combining the results of the 2 peak calling algorithms are shown. Then, the 4C results from this region for those of the 11 baits that were chosen for which the 4C experiment was successful are shown. Bait 19 is the promoter of the gene *CNNM2*, and bait 29 is the promoter of the gene *RPEL1*. Next, our previously published RNA sequencing data are shown.[5] Last, the graph shows the 8 putative enhancers that were selected in this region because of their interaction with the promoters of *CNNM2* and *RPEL1*.
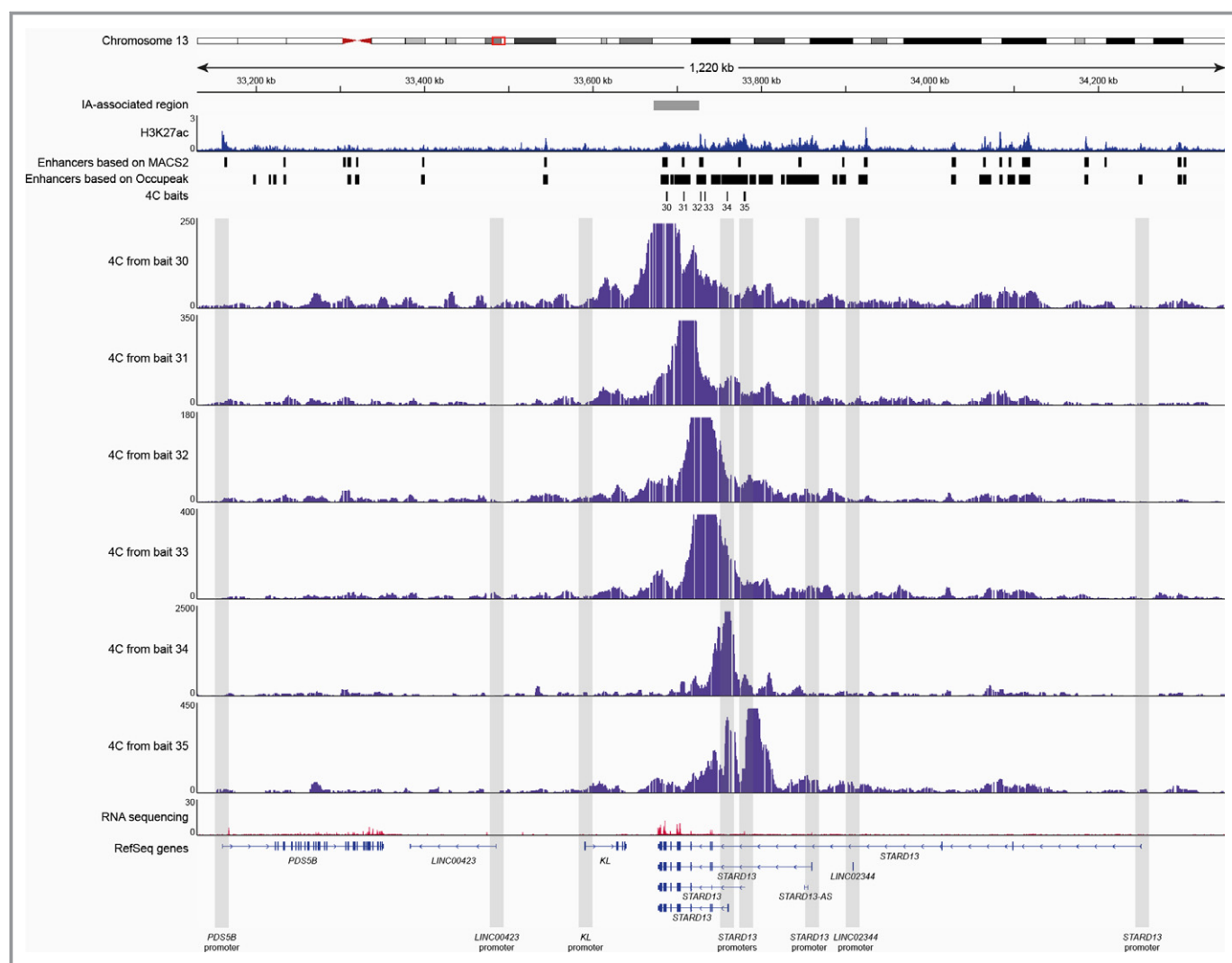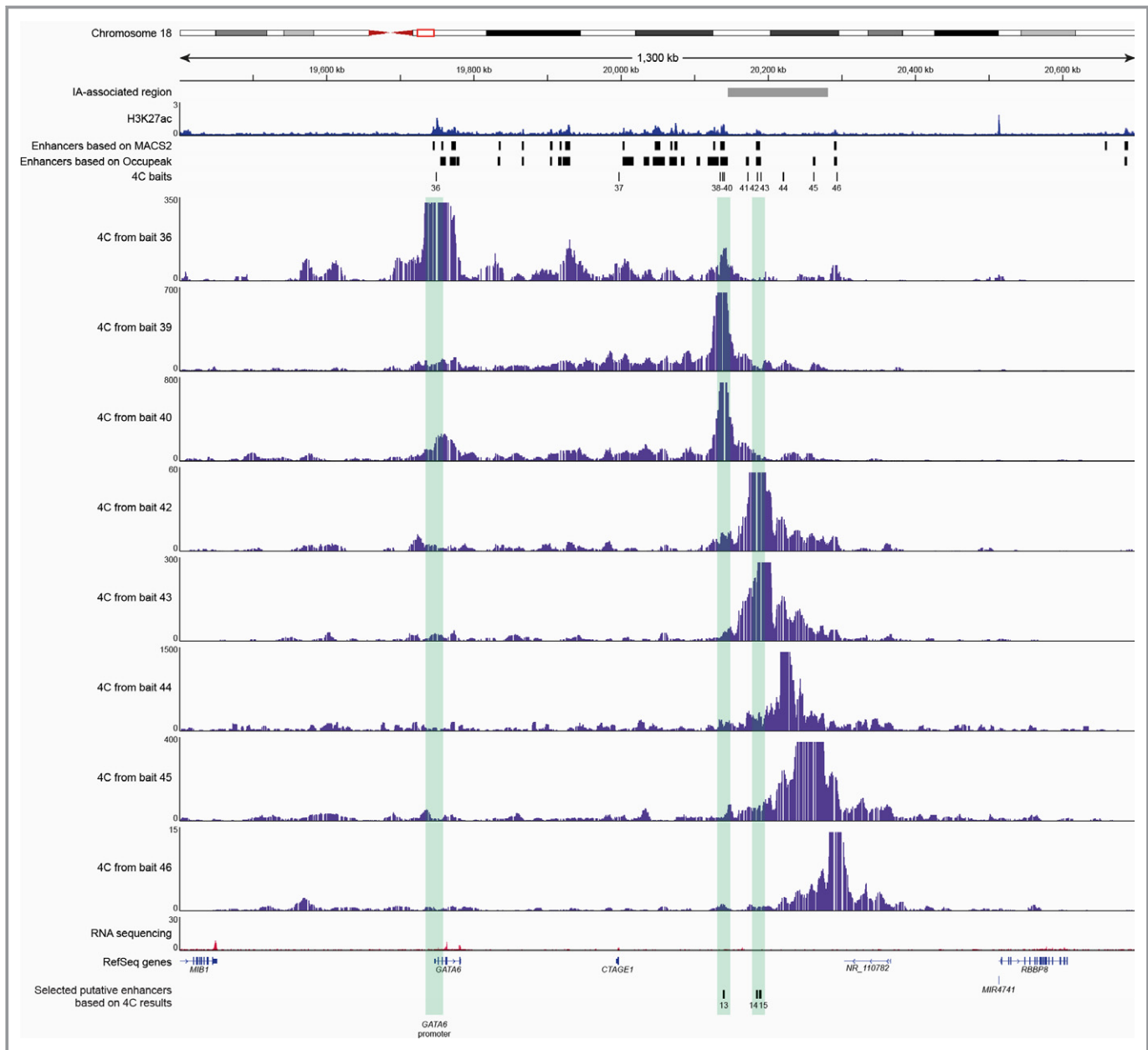
Figure 6. Chromosomal interactions around the intracranial aneurysm (IA)–associated region on chromosome 13. Genome browser view of a 1220 kilobase example region on chromosome 13, which contains an IA-associated region. This graph shows a combination of multiple types of data. First, the localization of the IA-associated region on the chromosome is shown. Then, our previously published chromatin immunoprecipitation and sequencing data for histone modification H3K27ac are shown,[5] including the enhancer peaks called using peak calling algorithms MACS2[5] and OccuPeak.[7] Next, the chromatin conformation capture technology (4C) baits that were selected by combining the results of the 2 peak calling algorithms are shown. Then, the 4C results from this region are shown for those of the 6 baits that were chosen for which the 4C experiment was successful. Baits 34 and 35 are the promoters of 2 different transcripts of the gene *STARD13*. Next, our previously published RNA sequencing data are shown.[5] No putative enhancers were selected in this region because there was no evidence of interactions between enhancers and promoters.

expression in vivo in zebrafish embryos, confirming their intrinsic activity. Because our 4C data show that these putative enhancers are in contact with the promoter of a nearby gene, this suggests that a SNP in these putative enhancers could alter the expression of these gene(s). This potentially links the identified IA-associated SNPs to altered gene expression involved in IA pathogenesis.

We identified physical contact between the promoter of *SOX17* and an active putative enhancer within the IA-associated region 8q11.23, 60 kb upstream of *SOX17*. *SOX17* is a likely candidate gene for IA because it is

expressed in endothelial cells, and a *SOX17* deficiency in mice induces IAs.[14]

We did not find evidence of physical contact between any putative enhancer within the IA-associated region on chromosome 9 and the promoter of previously suggested candidate gene *CDKN2B-AS* or *ANRIL*, a long-noncoding RNA gene.[15] In contrast, we did find evidence of contact between an active putative enhancer within this IA-associated region and 2 other genes that are expressed in the CoW, *MTAP* and *CDKN2B* (putative enhancers 75 kb upstream of *CDKN2B* and 280 kb downstream of *MTAP*), suggesting

Figure 7. Chromosomal interactions around the intracranial aneurysm (IA)–associated region on chromosome 18. Genome browser view of a 1300 kilobase example region on chromosome 18, which contains an IA-associated region. This graph shows a combination of multiple types of data. First, the localization of the IA-associated region on the chromosome is shown. Then, our previously published chromatin immunoprecipitation and sequencing data for histone modification H3K27ac are shown,[5] including the enhancer peaks called using peak calling algorithms MACS2[5] and OccuPeak.[7] Next, the chromatin conformation capture technology (4C) baits that were selected by combining the results of the 2 peak calling algorithms are shown. Then, the 4C results from this region are shown for those of the 11 baits that were chosen for which the 4C experiment was successful. Bait 36 is the promoter of the gene *GATA6*. Next, our previously published RNA sequencing data are shown.[5] Last, the graph shows the 3 putative enhancers that were selected in this region because of their interaction with the promoter of *GATA6*.

involvement of these genes in IA. *MTAP* homozygous-deficient mice die early during embryogenesis, whereas *MTAP* heterozygous mice have a reduced lifespan with defects in multiple organs.[16] The role of *MTAP* in the vasculature, however, is thus far unknown. Loss of *CDKN2B* increases VSMC apoptosis and results in the formation of aortic

aneurysms in mice.[17] The loss of VSMCs in *CDKN2B* knockout mice may explain its involvement in IAs because IAs have decreased vessel wall integrity related to a loss of VSMCs.[18]

Our results provide evidence of physical contact between the promoter of *CNNM2* (locus 10q24.32) and multiple

Table 3. Selected Enhancers for Testing in Enhancer Reporter Vector in Zebrafish

Putative Enhancer No.	Genomic Coordinates	Interaction With Promoter of Gene
1	Chromosome 8: 55306508-55309340	*SOX17*
2	Chromosome 9: 22079012-22081464	*MTAP* and *CDKN2B*
3	Chromosome 9: 22083188-22085645	*MTAP* and *CDKN2B*
4	Chromosome 9: 22117140-22119074	*MTAP* and *CDKN2B*
5	Chromosome 10: 104780000-104783499	*CNNM2*
6	Chromosome 10: 104797968-104799025	*CNNM2* and *RPEL1*
7	Chromosome 10: 104799792-104803919	*CNNM2* and *RPEL1*
8	Chromosome 10: 104804093-104805772	*CNNM2* and *RPEL1*
9	Chromosome 10: 104813022-104815607	*CNNM2* and *RPEL1*
10	Chromosome 10: 104828907-104831256	*CNNM2* and *RPEL1*
11	Chromosome 10: 104880183-104882307	*CNNM2* and *RPEL1*
12	Chromosome 10: 104884027-104887002	*CNNM2* and *RPEL1*
13	Chromosome 18: 20138725-20140673	*GATA6*
14	Chromosome 18: 20183875-20186066	*GATA6*
15	Chromosome 18: 20188536-20190356	*GATA6*

intrinsically active putative enhancers within the IA-associated region on this chromosome, between 120 and 200 kb downstream of the *CNNM2* promoter. *CNNM2* is a transmembrane protein that plays an important role in magnesium homeostasis. Mutations in *CNNM2* lead to hypomagnesemia,[19] a low concentration of magnesium in the blood. In addition, a GWAS links a SNP just 3' of *CNNM2* to blood pressure and hypertension.[20,21] Therefore, changes in *CNNM2* expression, induced by changes in enhancer sequences, could alter magnesium levels in the blood and lead to hypertension. Because hypertension is a strong risk factor for IAs[22] and aneurysmal subarachnoid hemorrhages,[23] this might explain the involvement of *CNNM2* in IA. We have also found evidence of physical contact between multiple intrinsically active putative enhancers in this locus and the gene *RPEL1* (between 125 and 210 kb upstream of the

promoter), which encodes a ribulose-5-phosphatase-3-epimerase. However, the role of this gene in IA remains unknown.

We found evidence of physical contact between the promoter of *GATA6* (locus 18q11.2) and an active putative enhancer 440 kb downstream. *GATA6* is expressed in VSMCs, and a conditional knockout of *GATA6* in VSMCs results in perinatal mortality from a spectrum of cardiovascular defects.[24] Other studies have suggested that *GATA6* plays a role in the contractility of VSMCs.[25–27] A loss of VSMC contractility in the CoW could lead to a weakening of the vessel wall and, thereby, increase the likelihood of IA development. Previous studies have already shown loss of VSMCs and changes in VSMC proliferation in IAs, further underlining the potential role of VSMCs in IA.[28]

The ISH experiments suggest that, together, the candidate target genes are expressed in all 3 major cell types of the vascular wall, indicating that multiple cell types in the CoW vessel wall may be involved in IA. In addition, we also saw that all genes are expressed in the intima. Although the intima consists mainly of endothelial cells, cells from other layers can infiltrate the intima[29] and endothelial cells can transition to mesenchymal cells, such as fibroblasts,[30] especially in atherosclerotic lesions. Because most of the CoW sections that were used in this study contained a thickened intima, suggestive of atherosclerosis,[13] the intimal expression found for some genes may be attributable to cells from other layers infiltrating the intima.
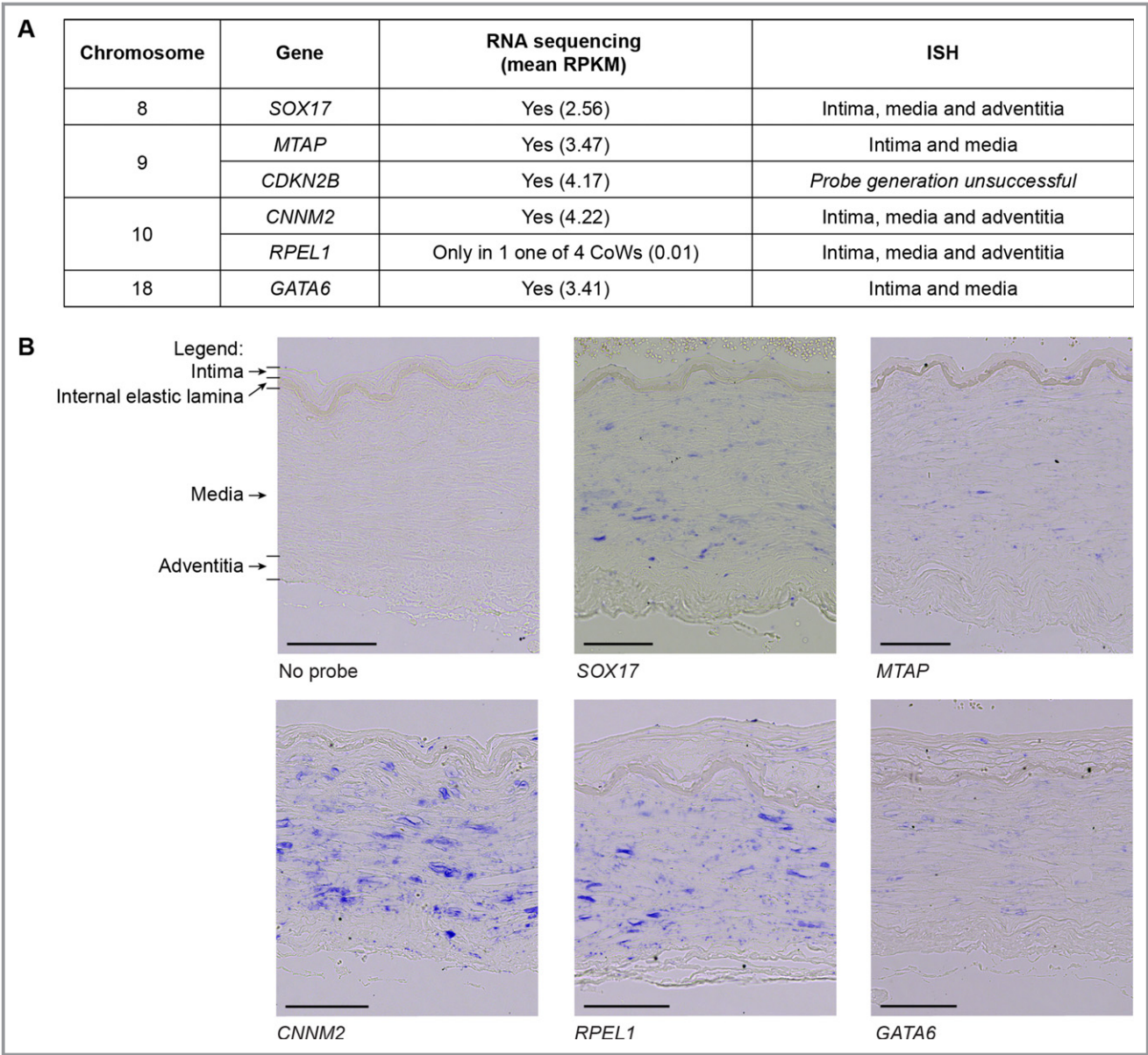
We have used 4C technology as a method to identify preferred contacts between putative enhancers and promoters. Physical contacts between putative enhancers and genes do not automatically imply that they functionally interact, but 4C technology enables prioritizing genes and putative enhancers for further analysis. We used the 4C results to further investigate whether the prioritized putative enhancers were able to induce GFP expression in a zebrafish reporter assay and whether the prioritized target genes were expressed in the CoW, additional criteria to evaluate their relevance. More important, 8 of 11 tested enhancers were able to induce GFP expression and all 6 prioritized genes are expressed in the CoW. Unambiguous demonstration that they are functionally wired and that variants in the enhancers affect the expression of these genes needs to come from editing experiments that delete or modify these enhancers in their natural context.

The role of regulatory DNA in disease is a subject of growing interest.[31–33] With this study, we started investigating the role that enhancers, a subset of regulatory regions, play in IA. We identified putative enhancers in IA-associated regions that contact nearby promoters and display intrinsic enhancer activity in vivo. Future studies should further investigate the role of these putative enhancers in IA and the effect of SNPs on their intrinsic activity, by comparing the in vivo activity of these putative enhancers obtained from
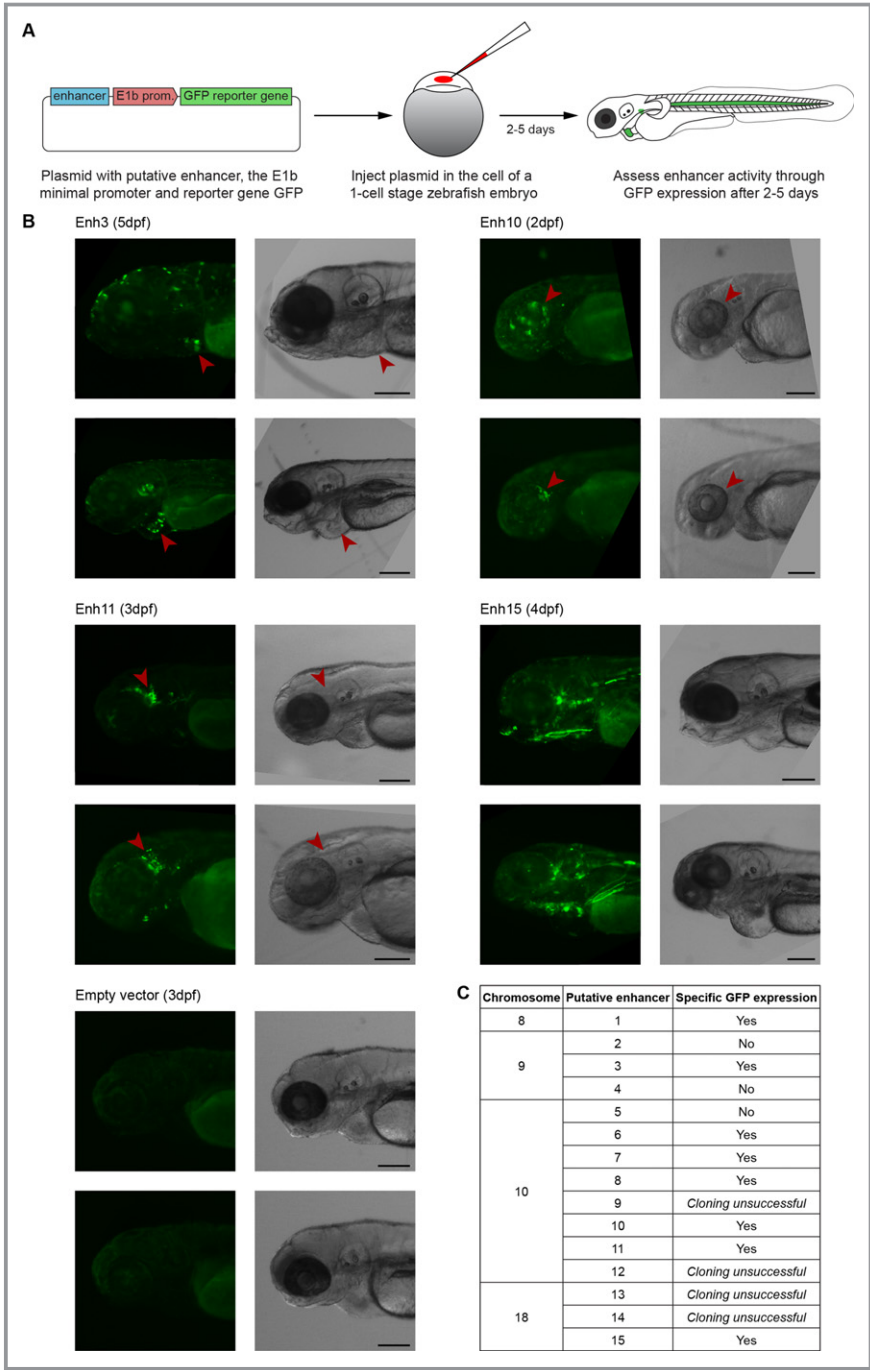
Figure 8. Selected human putative enhancers display intrinsic enhancer activity in vivo. **A**, Graphical representation of experimental setup. Plasmids in which the selected putative enhancer is followed by a minimal promoter and a green fluorescent protein (GFP) reporter gene were injected in the cell of a 1-cell stage zebrafish embryo. After 2 to 5 days of development, enhancer activity was assessed through GFP expression in these embryos. **B**, GFP fluorescence and bright-field images of injected zebrafish embryos between 2 and 5 days postfertilization (dpf) are shown. Enhancer activity resulted in clear GFP expression for enhancer 3 (Enh3; heart; arrowheads), Enh10 (eye; arrowheads), Enh11 (between the eye and ear; arrowheads), and Enh15 (multiple tissues), but no clear GFP expression was detected in embryos injected with the empty vector. Bar=200 μm. **C**, Table that summarizes the findings for all injected putative enhancers in each of the intracranial aneurysm–associated regions on the different chromosomes. For 4 putative enhancers, cloning was unsuccessful because of technical failure.

A

Chromosome	Gene	RNA sequencing (mean RPKM)	ISH
8	SOX17	Yes (2.56)	Intima, media and adventitia
9	MTAP	Yes (3.47)	Intima and media
	CDKN2B	Yes (4.17)	*Probe generation unsuccessful*
10	CNNM2	Yes (4.22)	Intima, media and adventitia
	RPEL1	Only in 1 one of 4 CoWs (0.01)	Intima, media and adventitia
18	GATA6	Yes (3.41)	Intima and media

B

Figure 9. Expression of potential candidate genes in the circle of Willis (CoW). **A**, Summary of the expression of investigated genes in this study, both from our previously published RNA-seq (RNA sequencing) data[5] in RPKM (Reads Per Kilobase Million) and from in situ hybridization (ISH) on CoW paraffin sections. For one ISH experiment, probe generation was unsuccessful because of technical failure. **B**, ISH on CoW paraffin sections shows that our potential candidate genes are expressed in the CoW. No probe represents the negative control. Bar=100 μm.

healthy individuals with the activity of the same enhancers obtained from patients carrying the risk allele. Finally, the role of the identified potential candidate genes (*SOX17*, *CDKN2B*, *MTAP*, *CNNM2*, *RPEL1*, and *GATA6*) in IA pathogenesis should be studied with the use of animal models for these genes.

Summary

In this study, we identified potential candidate genes that may play a role in IA: *SOX17*, *CDKN2B*, *MTAP*, *CNNM2*, *RPEL1*, and *GATA6*. This is based on the identification of putative

enhancers in IA-associated regions that exhibit intrinsic enhancer activity in vivo and physical contact between these putative enhancers and the promoters of the suggested candidate genes. These candidate genes are expressed in the CoW vessel wall. The suggested candidate genes should be studied in animal models to further elucidate their involvement in IA pathogenesis.

Acknowledgments

Sources of Funding

Disclosures

De Laat is founder of and shareholder of Cergentis.

References

1. Nieuwkamp DJ, Setz LE, Algra A, Linn FHH, De Rooij NK, Rinkel GJE. Changes in case fatality of aneurysmal subarachnoid haemorrhage over time, according to age, sex, and region: a meta-analysis. *Lancet Neurol*. 2009;8:635–642.

2. Bilguvar K, Yasuno K, Niemelä M, Ruigrok YM, von und zu Fraunberg M, van Duijn CM, van den Berg LH, Mane S, Mason CE, Choi M, Gaál E, Bayri Y, Kolb L, Arlier Z, Ravuri S, Ronkainen A, Tajima A, Laakso A, Hata A, Kasuya H, Koivisto T, Rinne J, Öhman J, Breteler MMB, Wijmenga C, State MW, Rinkel GJE, Hernesniemi J, Jääskeläinen JE, Palotie A, Inoue I, Lifton RP, Günel M. Susceptibility loci for intracranial aneurysm in European and Japanese populations. *Nat Genet*. 2008;40:1472–1477.

3. Yasuno K, Bilguvar K, Bijlenga P, Low S-K, Krischek B, Auburger G, Simon M, Krex D, Arlier Z, Nayak N, Ruigrok YM, Niemelä M, Tajima A, von und zu Fraunberg M, Dóczi T, Wirjatijasa F, Hata A, Blasco J, Oszvald A, Kasuya H, Zilani G, Schoch B, Singh P, Stüer C, Risselada R, Beck J, Sola T, Ricciardi F, Aromaa A, Illig T, Schreiber S, van Duijn CM, van den Berg LH, Perret C, Proust C, Roder C, Ozturk AK, Gaál E, Berg D, Geisen C, Friedrich CM, Summers P, Frangi AF, State MW, Wichmann HE, Breteler MMB, Wijmenga C, Mane S, Peltonen L, Elio V, Sturkenboom MCJM, Lawford P, Byrne J, Macho J, Sandalcioglu EI, Meyer B, Raabe A, Steinmetz H, Rüfenacht D, Jääskeläinen JE, Hernesniemi J, Rinkel GJE, Zembutsu H, Inoue I, Palotie A, Cambien F, Nakamura Y, Lifton RP, Günel M. Genome-wide association study of intracranial aneurysm identifies three new risk loci. *Nat Genet*. 2010;42:420–425.

4. Yasuno K, Bakırcıoğlu M, Low S-K, Bilgüvar K, Gaál E, Ruigrok YM, Niemelä M, Hata A, Bijlenga P, Kasuya H, Jääskeläinen JE, Krex D, Auburger G, Simon M, Krischek B, Ozturk AK, Mane S, Rinkel GJE, Steinmetz H, Hernesniemi J, Schaller K, Zembutsu H, Inoue I, Palotie A, Cambien F, Nakamura Y, Lifton RP, Günel M. Common variant near the endothelin receptor type A (EDNRA) gene is associated with intracranial aneurysm risk. *Proc Natl Acad Sci*. 2011;108:19707–19712.

5. Laarman MD, Vermunt MW, Kleinloog R, de Boer-Bergsma JJ, Brain Bank N, Rinkel GJE, Creyghton MP, Mokry M, Bakkers J, Ruigrok YM. Intracranial aneurysm-associated single-nucleotide polymorphisms alter regulatory DNA in the human circle of Willis. *Stroke*. 2018;49:447–453.

6. Ward LD, Kellis M. HaploReg: a resource for exploring chromatin states, conservation, and regulatory motif alterations within sets of genetically linked variants. *Nucleic Acids Res*. 2012;40:930–934.

7. De Boer BA, Van Duijvenboden K, Van Den Boogaard M, Christoffels VM, Barnett P, Ruijter JM. OccuPeak: ChIP-seq peak calling based on internal background modelling. *PLoS One*. 2014;9:1–15.

8. Van De Werken HJG, De Vree PJP, Splinter E, Holwerda SJB, Klous P, De Wit E, De Laat W. 4C technology: protocols and data analysis. *Methods Enzymol*. 2012;513:89–112.

9. Splinter E, de Wit E, van de Werken HJG, Klous P, de Laat W. Determining long-range chromatin interactions for selected genomic sites using 4C-seq technology: from fixation to computation. *Methods*. 2012;58:221–230.

10. Li Q, Ritter D, Yang N, Dong Z, Li H, Chuang JH, Guo S. A systematic approach to identify functional motifs within vertebrate developmental enhancers. *Dev Biol*. 2010;337:484–495.

11. Wu CC, Kruse F, Vasudevarao MD, Junker JP, Zebrowski DC, Fischer K, Noël ES, Grün D, Berezikov E, Engel FB, Van Oudenaarden A, Weidinger G, Bakkers J. Spatially resolved genome-wide transcriptional profiling identifies bmp signaling as essential regulator of zebrafish cardiomyocyte regeneration. *Dev Cell*. 2016;36:36–49.

12. Visel A, Minovitsky S, Dubchak I, Pennacchio LA. VISTA Enhancer Browser—a database of tissue-specific human enhancers. *Nucleic Acids Res*. 2007;35:88–92.

13. Aziz M, Yadav KS. Pathogenesis of atherosclerosis. *Med Clin Rev*. 2016;2:1–6.

14. Lee S, Kim IK, Ahn JS, Woo D-C, Kim S-T, Song S, Koh GY, Kim H-S, Jeon BH, Kim I. Deficiency of endothelium-specific transcription factor Sox17 induces intracranial aneurysm. *Circulation*. 2015;131:995–1005.

15. Che J. Molecular mechanisms of the intracranial aneurysms and their association with the long noncoding ribonucleic acid ANRIL—a review of literature. *Neurol India*. 2017;65:718–728.

16. Kadariya Y, Yin B, Tang B, Shinton SA, Quinlivan EP, Hua X, Klein-Szanto A, Al-Saleem TI, Bassing CH, Hardy RR, Kruger WD. Mice heterozygous for germ-line mutations in methylthioadenosine phosphorylase (MTAP) die prematurely of T-cell lymphoma. *Cancer Res*. 2009;69:5961–5969.

17. Leeper NJ, Raiesdana A, Kojima Y, Kundu RK, Cheng H, Maegdefessel L, Toh R, Ahn G-O, Ali ZA, Anderson DR, Miller CL, Roberts SC, Spin JM, de Almeida PE, Wu JC, Xu B, Cheng K, Quertermous M, Kundu S, Kortekaas KE, Berzin E, Downing KP, Dalman RL, Tsao PS, Schadt EE, Owens GK, Quertermous T. Loss of CDKN2B promotes p53-dependent smooth muscle cell apoptosis and aneurysm formation. *Arterioscler Thromb Vasc Biol*. 2013;33:e1–e10.

18. Frösen J. Smooth muscle cells and the formation, degeneration, and rupture of saccular intracranial aneurysm wall: a review of current pathophysiological knowledge. *Transl Stroke Res*. 2014;5:347–356.

19. de Baaij JHF, Hoenderop JGJ, Bindels RJM. Magnesium in man: implications for health and disease. *Physiol Rev*. 2015;95:1–46.

20. Newton-Cheh C, Johnson T, Gateva V, Tobin MD, Bochud M, Coin L, Najjar SS, Zhao JH, Heath SC, Eyheramendy S, Papadakis K, Voight BF, Scott LJ, Zhang F, Farrall M, Tanaka T, Wallace C, Chambers JC, Khaw K-T, Nilsson P, van der Harst P, Polidoro S, Grobbee DE, Onland-Moret NC, Bots ML, Wain LV, Elliott KS, Teumer A, Luan J, Lucas G, Kuusisto J, Burton PR, Hadley D, McArdle WL; Wellcome Trust Case Control Consortium, Brown M, Dominiczak A, Newhouse SJ, Samani NJ, Webster J, Zeggini E, Beckmann JS, Bergmann S, Lim N, Song K, Vollenweider P, Waeber G, Waterworth DM, Yuan X, Groop L, Orho-Melander M, Allione A, Di Gregorio A, Guarrera S, Panico S, Ricceri F, Romanazzi V, Sacerdote C, Vineis P, Barroso I, Sandhu MS, Luben RN, Crawford GJ, Jousilahti P, Perola M, Boehnke M, Bonnycastle LL, Collins FS, Jackson AU, Mohlke KL, Stringham HM, Valle TT, Willer CJ, Bergman RN, Morken MA, Döring A, Gieger C, Illig T, Meitinger T, Org E, Pfeufer A, Wichmann HE, Kathiresan S, Marrugat J, O'Donnell CJ, Schwartz SM, Siscovick DS, Subirana I, Freimer NB, Hartikainen A-L, McCarthy MI, O'Reilly PF, Peltonen L, Pouta A, de Jong PE, Snieder H, van Gilst WH, Clarke R, Goel A, Hamsten A, Peden JF, Seedorf U, Syvänen A-C, Tognoni G, Lakatta EG, Sanna S, Scheet P, Schlessinger D, Scuteri A, Dörr M, Ernst F, Felix SB, Homuth G, Lorbeer R, Reffelmann T, Rettig R, Völker U, Galan P, Gut IG, Hercberg S, Lathrop GM, Zelenika D, Deloukas P, Soranzo N, Williams FM, Zhai G, Salomaa V, Laakso M, Elosua R, Forouhi NG, Völzke H, Uiterwaal CS, van der Schouw YT, Numans ME, Matullo G, Navis G, Berglund G, Bingham SA, Kooner JS, Connell JM, Bandinelli S, Ferrucci L, Watkins H, Spector TD, Tuomilehto J, Altshuler D, Strachan DP, Laan M, Meneton P, Wareham NJ, Uda M, Jarvelin M-R, Mooser V, Melander O, Loos RJF, Elliott P, Abecasis GR, Caulfield M, Munroe PB. Genome-wide association study identifies eight loci associated with blood pressure. *Nat Genet*. 2009;41:666–676.

21. Takeuchi F, Isono M, Katsuya T, Yamamoto K, Yokota M, Sugiyama T, Nabika T, Fujioka A, Ohnaka K, Asano H, Yamori Y, Yamaguchi S, Kobayashi S, Takayanagi R, Ogihara T, Kato N. Blood pressure and hypertension are associated with 7 loci in the Japanese population. *Circulation*. 2010;121:2302–2309.

22. Vlak MHM, Rinkel GJE, Greebe P, Algra A. Independent risk factors for intracranial aneurysms and their joint effect: a case-control study. *Stroke*. 2013;44:984–987.

23. Vlak MHM, Rinkel GJE, Greebe P, Greving JP, Algra A. Lifetime risks for aneurysmal subarachnoid haemorrhage: multivariable risk stratification. *J Neurol Neurosurg Psychiatry*. 2013;84:619–623.

24. Lepore JJ, Mericko PA, Cheng L, Lu MM, Morrisey EE, Parmacek MS. GATA-6 regulates semaphorin 3C and is required in cardiac neural crest for cardiovascular morphogenesis. *J Clin Invest*. 2006;116:929–939.

25. Perlman H, Suzuki E, Simonson M, Smith RC, Walsch K. GATA-6 induces p21 Cip1 expression and G1 cell cycle arrest. *J Biol Chem*. 1998;273:13713–13718.

26. Chang DF, Belaguli NS, Iyer D, Roberts WB, Wu S-P, Dong X-R, Marx JG, Moore MS, Beckerle MC, Majesky MW, Schwartz RJ. Cysteine-rich LIM-only proteins CRP1 and CRP2 are potent smooth muscle differentiation cofactors. *Dev Cell*. 2003;4:107–118.

27. Mano T, Luo Z, Malendowicz SL, Evans T, Walsh K. Reversal of GATA-6 downregulation promotes smooth muscle differentiation and inhibits intimal hyperplasia in balloon-injured rat carotid artery. *Circ Res*. 1999;84:647–654.

28. Chalouhi N, Ali MS, Jabbour PM, Tjoumakaris SI, Gonzalez LF, Rosenwasser RH, Koch WJ, Dumont AS. Biology of intracranial aneurysms: role of inflammation. *J Cereb Blood Flow Metab*. 2012;32:1659–1676.

29. Wang D, Wang Z, Zhang L, Wang Y. Roles of cells from the arterial vessel wall in atherosclerosis. *Mediators Inflamm*. 2017;2017:ID 8135934.

30. Evrard SM, Lecce L, Michelis KC, Nomura-Kitabayashi A, Pandey G, Purushothaman K-R, D'Escamard V, Li JR, Hadri L, Fujitani K, Moreno PR, Benard L, Rimmele P, Cohain A, Mecham B, Randolph GJ, Nabel EG, Hajjar R, Fuster V, Boehm M, Kovacic JC. Endothelial to mesenchymal transition is common in atherosclerotic lesions and is associated with plaque instability. *Nat Commun*. 2016;7:11853.

31. Huang Q. Genetic study of complex diseases in the post-GWAS era. *J Genet Genomics*. 2015;42:87–98.

32. Albert FW, Kruglyak L. The role of regulatory variation in complex traits and disease. *Nat Rev Genet*. 2015;16:197–212.

33. Visscher PM, Wray NR, Zhang Q, Sklar P, McCarthy MI, Brown MA, Yang J. 10 Years of GWAS discovery: biology, function, and translation. *Am J Hum Genet*. 2017;101:5–22.

SUPPLEMENTAL MATERIAL

Table S1. Characteristics of CoW donors and use of CoW tissue.

Sample	Sex	Age	Post-mortem delay (hours)	Cause of death	Relevant pathological findings	Experiments
CoW1	Female	92	06:35	Heart failure	-	4C
CoW2	Female	54	08:00	Acute renal failure	-	4C
CoW3	Female	60	08:25	Metastasized non-small cell lungcarcinoma, euthanasia	Adenocarcinoma metastases in cerebro	ISH probe synthesis
CoW4	Female	89	13:00	Voluntary euthanasia	-	ISH

CoW: circle of Willis, ISH: in situ hybridization, 4C: chromatin conformation capture based technique

Table S2. Primers for 4C experiments.

Bait	Putative enhancer / promoter	Selected based on	Reading primer	Non-reading primer	Fragment size
1	Putative enhancer	OccuPeak	TGTAAGAATTCTCTGTGATC	CTGACTGTTGACAAACATGC	266
2	Putative enhancer	OccuPeak	TTTTGATACTATGCTTGATC	CCACTGCTATGAACAATTGA	218
3	Putative enhancer	MACS2 and OccuPeak	TGAAACATTGTAAGGAGATC	CAAACACCTCACCAGACAC	1108
4	Promoter *EDNRA*	Enrichment in 4C from bait 2 and located in IA-associated region	TAGTGCAGGCAGATTTGATC	AGTTTTCTTTTTCGTGCGAG	339
5	Promoter *TMEM184C*	Enrichment in 4C from bait 4	TAGGCCGCTTGGTTATTTCT	GCACCTGCTCTTCTTTCTAA	361
6	Putative enhancer	MACS2 and OccuPeak	TTTCCTGACTTCTGCGGATC	CAGTTTGGTTCCCTGATTTA	417
7	Putative enhancer	OccuPeak	AGAAATTAACACAGAAGATC	AGGCAAAGGTATTGAACAGA	231
8	Putative enhancer	OccuPeak	AGATTTAGGAGGAATAGATC	CACTCACCCGTTGTTATCAC	221
9	Putative enhancer	OccuPeak	TGAGATTCTTATGTCTGATC	TAAAAGTGGTGCAAAACATG	209
10	Promoter *SOX17*	Enrichment in 4C from bait 8 and 9 and located between both IA-associated regions	ATTAAACTTGTGTTTCGATC	AAGGCTCACCTGTTACTGAA	290
11	Promoter *MTAP*	Enrichment in 4C from bait 15, 17 and 18	AATAATGGGTGGCAAGGATC	GAGTTGTGCAAGGTCTCAAC	350
12	Promoter *CDKN2B*	Enrichment in 4C from bait 13, 14, 15 and 16	CTAAAGCTTCACACTTGATC	ACCTGACAAAGTGGGTTTAA	1150
13	Putative enhancer	Enrichment in 4C from promoter CDKN2B	ATCTGAGGTGAATGTCGATC	AATCTGCCTGTTCATCAAAG	349
14	Putative enhancer	Enrichment in 4C from promoter CDKN2B	GGCTGGGTTTAGATAAATGG	TCATGAGAAAAATGGGAATC	188
15	Putative enhancer	MACS2 and OccuPeak	TGGTTTGGATTGTCAGGATC	TGATAAGAAAAGCTCACAAGC	519

16	Putative enhancer	MACS2 and OccuPeak	ACAGCAAATAAGAGGCGATC	AGTTTCATTGGAAATGGACA	479
17	Putative enhancer	Enrichment in 4C from promoter CDKN2B and MTAP	GCAAGAGTTGGAGAGAGATC	AAAGAAAATGAGGTAAGGCC	687
18	Putative enhancer	MACS2 and OccuPeak	CTGCCAAGAAGGCATGTGAT	TTCAATTAGCTGTGCGAATA	170
19	Promoter *CNNM2*	Enrichment in 4C from bait 21, 22, 23, and 24	TAGTCCAAACCTGGCCGGTC	CCTCGAGACTCCTAGGGTAC	304
20	Putative enhancer	MACS2 and OccuPeak	AAAGAAAGAATACTGAGATC	TCTTTTCCACTTGCAGATTT	869
21	Putative enhancer	MACS2 and OccuPeak	TATTCCTACCATGGCTGATC	ATTAGTCCATTTGCATTGCT	173
22	Putative enhancer	MACS2 and OccuPeak	GTCCCTTAAGCATAGACAGA	TGTCAAGTTTCACTGAGCTG	310
23	Putative enhancer	OccuPeak	ATATAAGAAAGCCATGGATC	AACTAAATTCCCAACAGTGC	348
24	Putative enhancer	MACS2 and OccuPeak	TTCAGGGACCCTCTGTGATC	TGGATACTCCGAATGTTCTT	504
25	Putative enhancer	MACS2 and OccuPeak	ACTGTCCTAAAACCCTGATC	TTCTCCGATATGTTCAAGCT	1682
26	Putative enhancer	MACS2 and OccuPeak	CAGAGAGGGACATATAGATC	ATGCATGGAGTTTGAAAGAG	252
27	Promoter *NT5C2*	Enrichment in 4C from bait 22 and 24	TGTTCCATCGTTTGAAGATC	AACACCAGCTTTGAAGTTTG	288
28	Putative enhancer	OccuPeak	CTTCTGAAACTCTGAAGATC	TAGGCACTCAAACGGATACT	250
29	Promoter *RPEL1*	Enrichment in 4C from bait 20, 22, 23 and 24	TTCAGGAAACCAATGCAGAA	TTCTTTGACATGCACATGAT	439
30	Putative enhancer	MACS2 and OccuPeak	GTGAGAGGACTAAAGTGATC	AAAATACTGATTGGGTGTGC	256
31	Putative enhancer	MACS2 and OccuPeak	ACCCTGTGCCTACAACGATC	TCATGGCACCTTGTGTATAA	638
32	Putative enhancer	MACS2 and OccuPeak	GTGTTCTTAACCTAGGGATC	CTACCAATTTCCAAGTGCTC	758
33	Putative enhancer	MACS2 and OccuPeak	AGTCATACCCGGGGTGGATC	GACAGGTCATGTGCTCTACA	402

34	Promoter *STARD13*	Enrichment in 4C from bait 31	TCTAAGCGAAGGAGACAGTG	CATGCAAGGCTAAGTAACAA	409
35	Promoter *STARD13*	Enrichment in 4C from bait 32	AACCAGGCACACCATTGATC	CCACACGTTTACCATGAATA	847
36	Promoter *GATA6*	Enrichment in 4C from bait 40 and 42	TTTCTCTCCTCCCCTCGATC	CTGACCTTTGGGAACTTTAA	603
37	Promoter *CTAGE1*	Enrichment in 4C from bait 39	AAGCCGACTCGTAACTGATC	CTTTTGCAAGAAGCTGAAGT	564
38	Putative enhancer	MACS2 and OccuPeak	GAGAAGACCGTTCTAGGATC	AGCTGGTTGATTGCTTTTAG	639
39	Putative enhancer	MACS2 and OccuPeak	CCAGCTACCTAGTAAAGATC	GAAGGAAGTATGAATCGCTG	320
40	Putative enhancer	MACS2 and OccuPeak	GGGTGTCAGGGAAGAGGATC	AAACCCAGAAGAAAGGAAGT	305
41	Putative enhancer	OccuPeak	TGAAAGTGCTAAATGTGATC	AGTTGCAATTCAACGTCAGT	371
42	Putative enhancer	MACS2 and OccuPeak	TTGGGGCTCAAGTCCAGATC	TACTCCAAATGTATCCCTGG	322
43	Putative enhancer	MACS2 and OccuPeak	GCCTCTCATCCGTCAGGATC	AAAAGAGAAACTTTCCCCAC	484
44	Putative enhancer	Enrichment in 4C from putative enhancers 39, 42, 43 and 45	TAGTTTCCAGCAGGGAGATC	TCCAAATATTTTTGACCTGC	616
45	Putative enhancer	OccuPeak	GGAAGGAGAGCAGTGTGATC	TAAGTGTTCTTTTGGGCACT	435
46	Putative enhancer	MACS2 and OccuPeak	AGGTCAACTATTTTTGGATC	TTGGAAATGTCTTCTTGGTT	545

4C: chromosome conformation capture based technique, MACS2 and OccuPeak: two different peak calling algorithms.

Table S3. Quality assessment of 4C datasets.

Experiment	Mapped reads (#)	Unique reads (#)	Unique *cis* reads (#)	% *cis*/total reads	% fragends covered in 200kb around bait	Illumina sequencer used
Bait1	755	511	388	75.93	12.58	HiSeq2000
Bait2	985845	511817	261177	51.03	83.64	HiSeq2000
Bait3	784762	101070	72139	71.38	77.71	HiSeq2000
Bait4	1912946	1094979	787000	71.87	48.76	NextSeq500
Bait5	1371544	776302	567720	73.13	71.74	NextSeq500
Bait6	155042	93765	50533	53.89	70.78	HiSeq2000
Bait7	5882	4452	2739	61.52	30.38	HiSeq2000
Bait9	444991	237082	119489	50.40	69.66	HiSeq2000
Bait10	550123	346810	259534	74.83	36.39	NextSeq500
Bait11	1332622	244454	166923	68.28	41.69	NextSeq500
Bait12	518001	349686	231756	66.28	54.77	NextSeq500
Bait13	548898	252950	170981	67.59	75.00	HiSeq2000
Bait14	878700	231613	158023	68.23	67.99	NextSeq500
Bait15	1498882	725451	378666	52.20	92.44	HiSeq2000
Bait16	38918	16078	11064	68.81	63.16	HiSeq2000
Bait17	623503	462548	250970	54.26	89.80	HiSeq2000
Bait18	1268250	818036	595339	72.78	75.91	NextSeq500
Bait19	1268062	460813	295385	64.1	52.99	NextSeq500
Bait20	290323	99313	62033	62.46	79.06	HiSeq2000
Bait21	102019	51655	30592	59.22	61.68	HiSeq2000
Bait22	1144578	236495	144550	61.12	68.00	NextSeq500
Bait23	301913	151624	93774	61.85	73.93	HiSeq2000
Bait24	71441	35944	23058	64.15	65.42	HiSeq2000
Bait25	76077	40561	24203	59.67	73.65	HiSeq2000
Bait26	21673	12350	7206	58.35	63.30	HiSeq2000
Bait27	1064460	585079	329590	56.33	78.13	NextSeq500
Bait28	1431445	704882	423212	60.04	75.71	HiSeq2000
Bait29	1444299	267995	167132	62.36	74.18	NextSeq500
Bait30	1443579	326316	223077	68.36	80.18	HiSeq2000
Bait31	519997	324978	221857	68.27	82.57	HiSeq2000
Bait32	227740	177263	121110	68.32	78.40	HiSeq2000
Bait33	762741	416211	286082	68.73	77.71	HiSeq2000
Bait34	1209762	558368	386610	69.24	73.21	NextSeq500
Bait35	737368	434569	293285	67.49	56.02	NextSeq500
Bait36	779627	559613	343459	61.37	42.36	NextSeq500
Bait37	999865	482525	71314	14.78	67.82	NextSeq500
Bait38	3704	1750	1176	67.2	28.19	HiSeq2000
Bait39	745333	541270	350656	64.78	72.97	HiSeq2000

Bait40	778315	588192	378495	64.35	72.30	HiSeq2000
Bait42	220089	59960	38067	63.49	59.11	HiSeq2000
Bait43	692046	244779	161096	65.81	68.89	HiSeq2000
Bait44	1656784	274341	178126	64.93	65.11	NextSeq500
Bait45	751997	524306	358965	68.46	80.77	HiSeq2000
Bait46	32925	11263	7430	65.97	56.85	HiSeq2000

cis reads: reads on the same chromosome as the bait, fragends: fragment ends, 4C: chromatin conformation capture based technique, red numbers do not meet quality criteria

Table S4. Primers used for testing enhancer activity in zebrafish.

Putative enhancer number	Forward primer	Reverse primer	PCR product size
1	CTGGCCATGTGAGGAGCAAT	AGCTGGAGACTTCCGAGCTA	3109
2	TCTTTTGGGTTTCCCCATTGTCT	TGCTCAGACCCACAACTTGTTC	2703
3	GCCATGCCCTGTACTAAGAACTA	AGTGACTCCAAGATACCCTGAGAT	2681
4	ATGGAAGCTGGGAGTGTTGAA	AATTGGAATGCTTGGCCTTGA	2307
5	CGAACATGTGTTACTCGTGTGG	AGGTTATGTGGAAGAAGTATGCAA	3982
6	TTGATGTCCTTGAGGGTAACCA	TGCCTTGCAAGTCTTCGGAC	1301
7	GAGGGTGGCATCAAGCTAGG	GCAGAAAAGCGACTCTGGGA	4441
8	TCGTTTTCCCAGAGTCGCTT	TACCCAGCAAAGACACTGCC	1920
9	Technical failure	Technical failure	-
10	AGTAAGGCCCCTCTCCTTTC	AGGAATACAGGGAGGCCAAGA	2829
11	AAGAAGAAATGCTAAAGCACAGACT	AAGTCGGGAGGTGAGAGTGA	2893
12	Technical failure	Technical failure	-
13	Technical failure	Technical failure	-
14	Technical failure	Technical failure	-
15	GTTCACCGTCTCTTACCGGG	TAGCAAATAGCTGACGGGCAA	2501

PCR: polymerase chain reaction

Table S5. Primers used to make antisense RNA probes for in situ hybridization.

| Gene	Control gene / gene of interest	Forward primer	Reverse primer	PCR product size
EDN1	Control - endothelium	GGCTGAAGGATCGCTTTGAG	TGGAAGCCAGTGAAGATGGT	953
VWF	Control - endothelium	AGGTGTCAGTGCTGCAGTAT	ATTCACCGTCACCTCCATGT	890
ACTA2	Control - smooth muscle	TGCCTTGGTGTGTGACAATG	CGATGAAGGATGGCTGGAAC	785
TAGLN	Control - smooth muscle	GGCTGGTGGAGTGGATCATA	CAGTGACAGAGCCTCAAAGC	649
FN1	Control - fibroblasts	AACGAAGGCTTGAACCAACC	TCGAAGCAGAACAGGCAATG	807
CDKN2B	Gene of interest	Technical failure	Technical failure	-
CNNM2	Gene of interest	CCAGCTCAATTCTTCGCTCC	CCCCACAGTGATGACAGACT	878
GATA6	Gene of interest	TGTGCAATGCTTGTGGACTC	CTCAGCCTCCAGAGATGTGT	863
MTAP	Gene of interest	GATTCAGCCCGGCGATATTG	GGGAGAAGAGAATGGTGGGT	827
RPEL1	Gene of interest	GTCGGGCTGCAAGATTGG	GATGGGAACTGGGTCCTCAA	501
SOX17	Gene of interest	GCATGACTCCGGTGTGAATC	TGCCACTTCCCAAGGTGTAA	927

PCR: polymerase chain reaction

Table S6. Identified contacts between putative enhancers and promoters for those enhancers selected for activity testing.

Selected enhancer	Enhancer bait #	Promoter bait # (gene)	Reciprocal confirmation of interaction
1	8	10 (*SOX17*)	No, 4C from bait 8 was unsuccessful, but increased contact frequency seen from *SOX17* promoter (bait 10)
2	13	12 (*CDKN2B*)	Yes, but strongest increase of contact frequency seen from *CDKN2B* promoter (bait 12)
3	14	12 (*CDKN2B*)	Yes, but strongest increase of contact frequency seen from *CDKN2B* promoter (bait 12)
4	17/18	11 (*MTAP*)	Yes
	17/18	12 (*CDKN2B*)	No
5	21	19 (*CNNM2*)	Yes
	21	29 (*RPEL1*)	No
6-8	22	19 (*CNNM2*)	Yes
	22	29 (*RPEL1*)	Yes
9	23	19 (*CNNM2*)	Yes
	23	29 (*RPEL1*)	Yes
10	24	19 (*CNNM2*)	Yes
	24	29 (*RPEL1*)	Yes
11-12	-	19 (*CNNM2*)	Not determined
	-	29 (*RPEL1*)	Not determined
13	39/40	36 (*GATA6*)	Yes
14-15	42/43	36 (*GATA6*)	Yes, but strongest increase of contact frequency seen from *GATA6* promoter (bait 36)

4C: chromatin conformation capture based technique

Figure S1. Selection of four additional putative enhancers based on chromatin conformation capture (4C) results from this study.
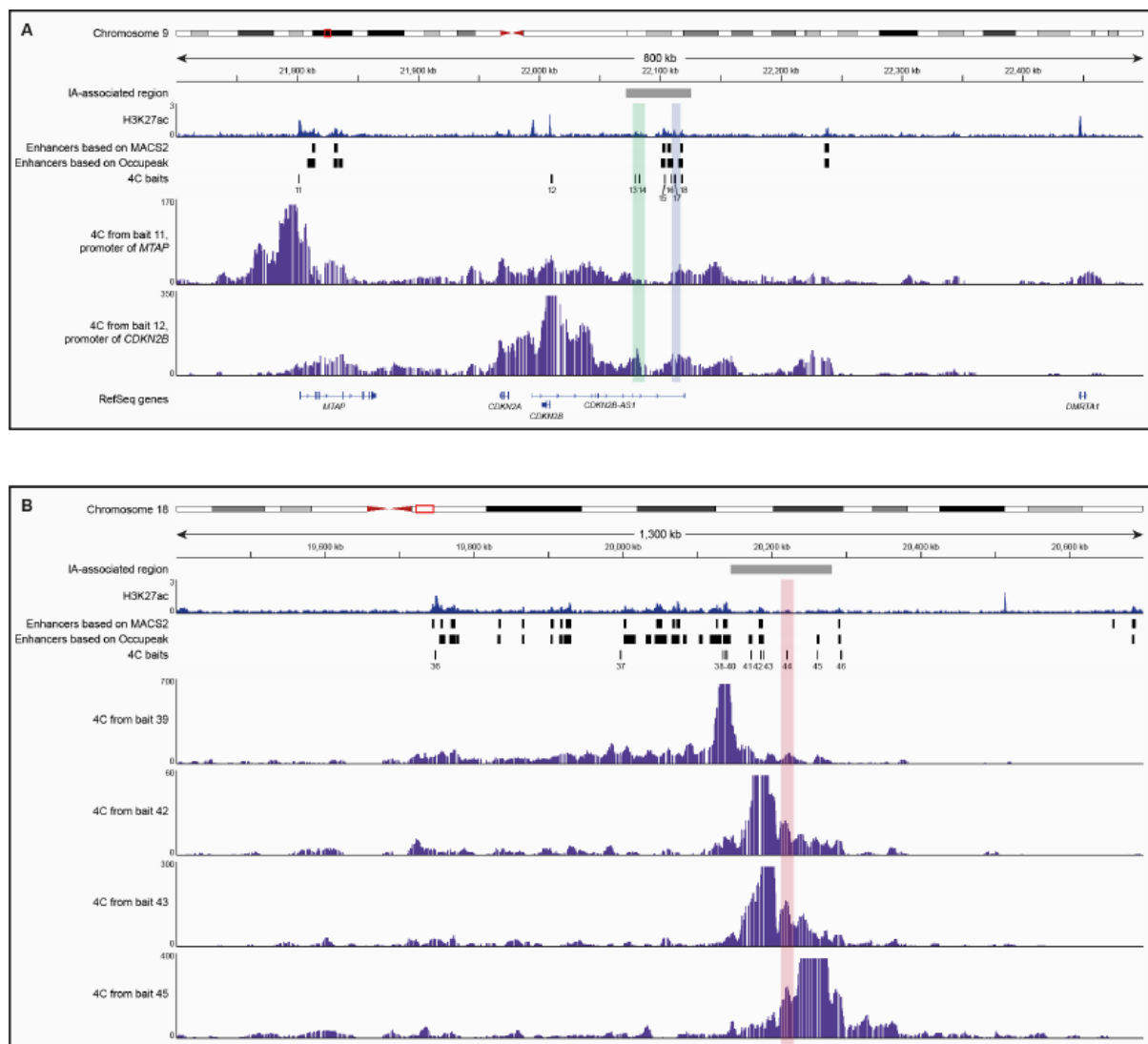
Both A and B show the intracranial aneurysm (IA)-associated region in each chromosome, the H3K27ac chromatin immunoprecipitation and sequencing (ChIP-seq) experiments in the CoW from our previous publication,[1] including the enhancer peaks called using peak calling algorithms MACS21 and Occupeak.[2] Next are the 4C baits that were selected. A, Selection of putative enhancers with bait numbers 13, 14 and 17. Bait 13 and 14 (green bar) were selected based on an enrichment of reads in the 4C experiment using the promoter of *CDKN2B* (bait 12) as a viewpoint, and based on a slight enrichment of reads in the H3K27ac (ChIP-seq) experiments. Bait 17 (blue bar) was selected based on an enrichment of reads in the 4C

experiments using *MTAP* (bait 11) and *CDKN2B* (bait 12) as a viewpoint, and based on a slight enrichment of reads in the H3K27ac (ChIP-seq) experiments. B, Selection of putative enhancer with bait number 44. Bait 44 (pink bar) was selected based on an enrichment of reads in the 4C experiments using putative enhancers with bait numbers 39, 42, 43 and 45 as a viewpoint, and based on a slight enrichment of reads in the H3K27ac (ChIP-seq) experiments.

Figure S2. Quality assessment of chromatin conformation capture (4C) datasets.
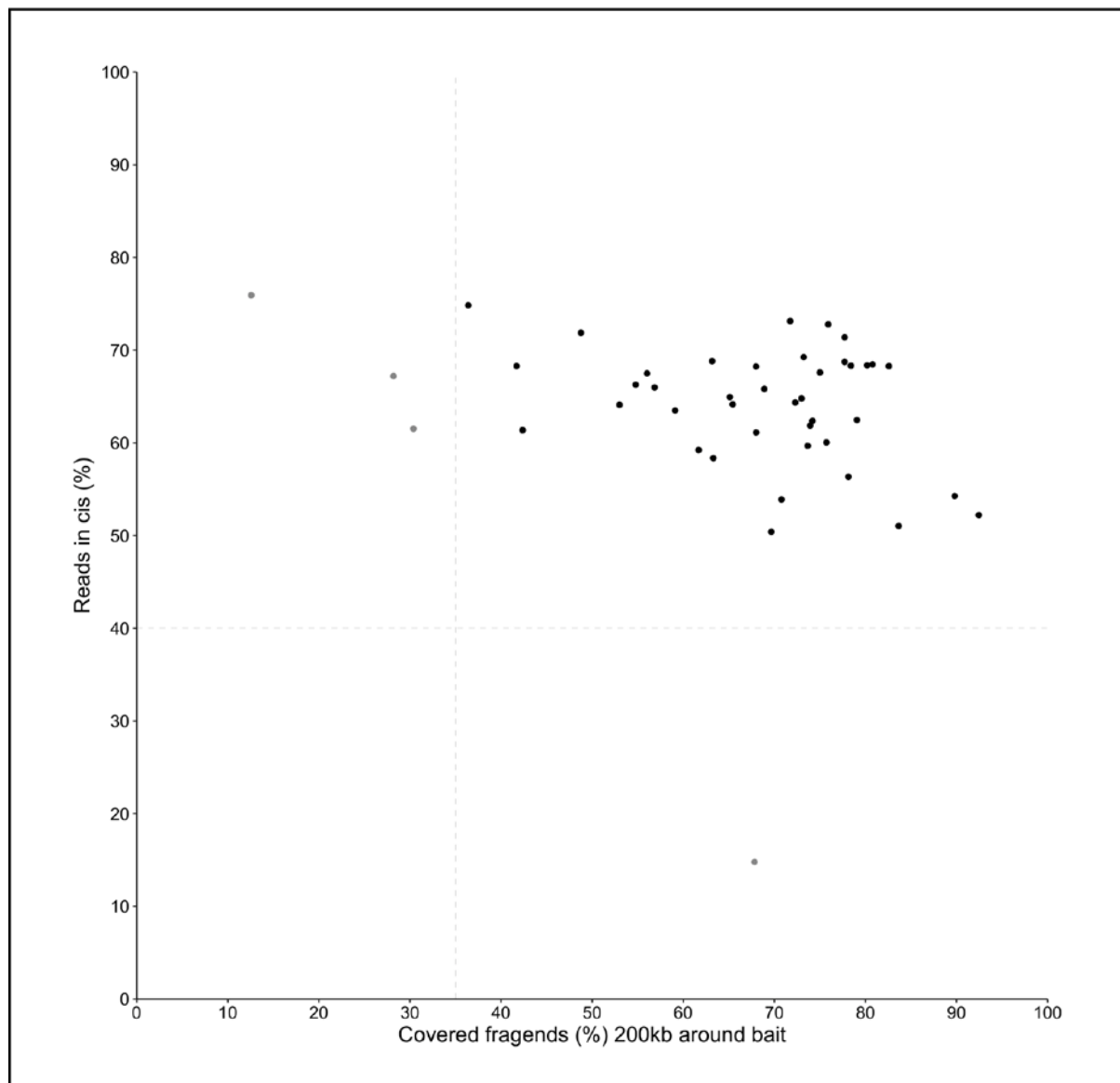
Each dot represents a dataset with the quality values for reads in *cis* versus total reads (%) on the y-axis and the percentage of covered fragends in the 200kb around the bait. Cut-off values of 40% for the reads in cis versus total reads and 35% for the percentage of covered fragends were used to include datasets in the study. From the 45 datasets, 4 datasets were removed from the analysis based because they did not meet the quality criteria.

Figure S3. Chromosomal interactions around the intracranial aneurysm (IA)-associated region on chromosome 4, including replicate.
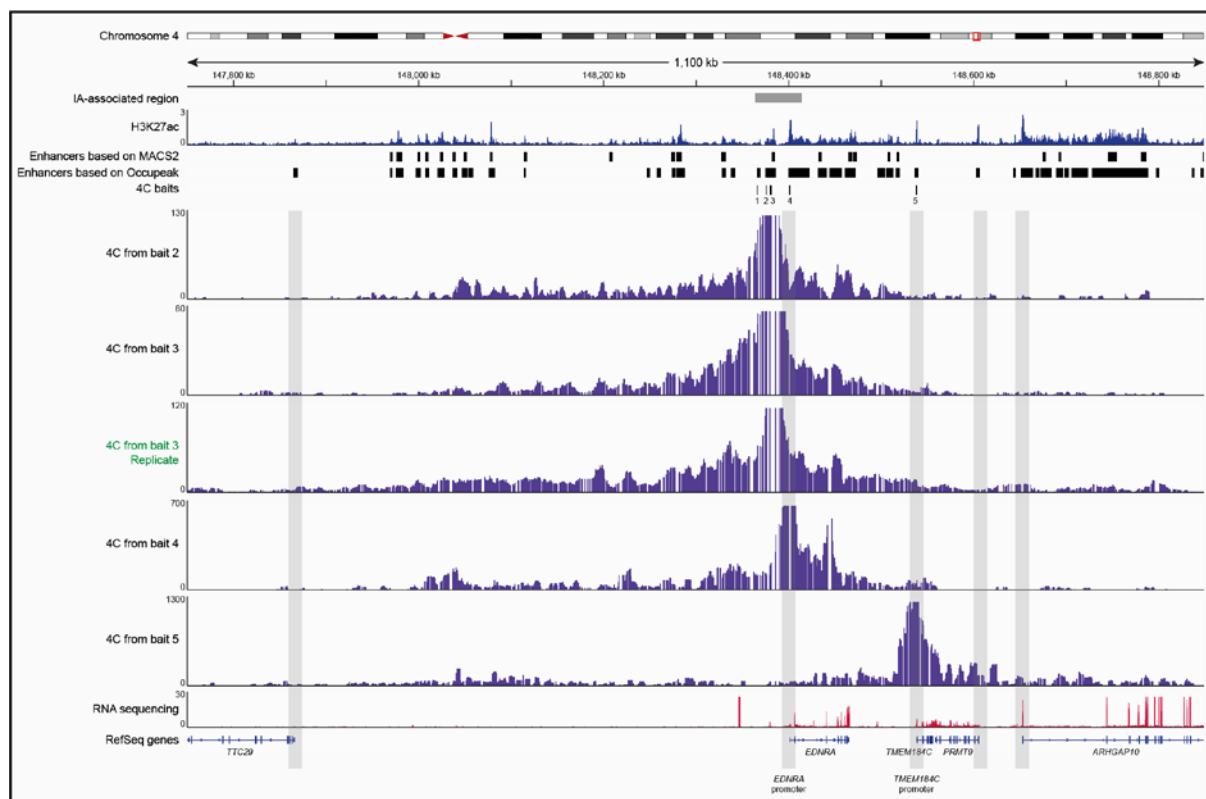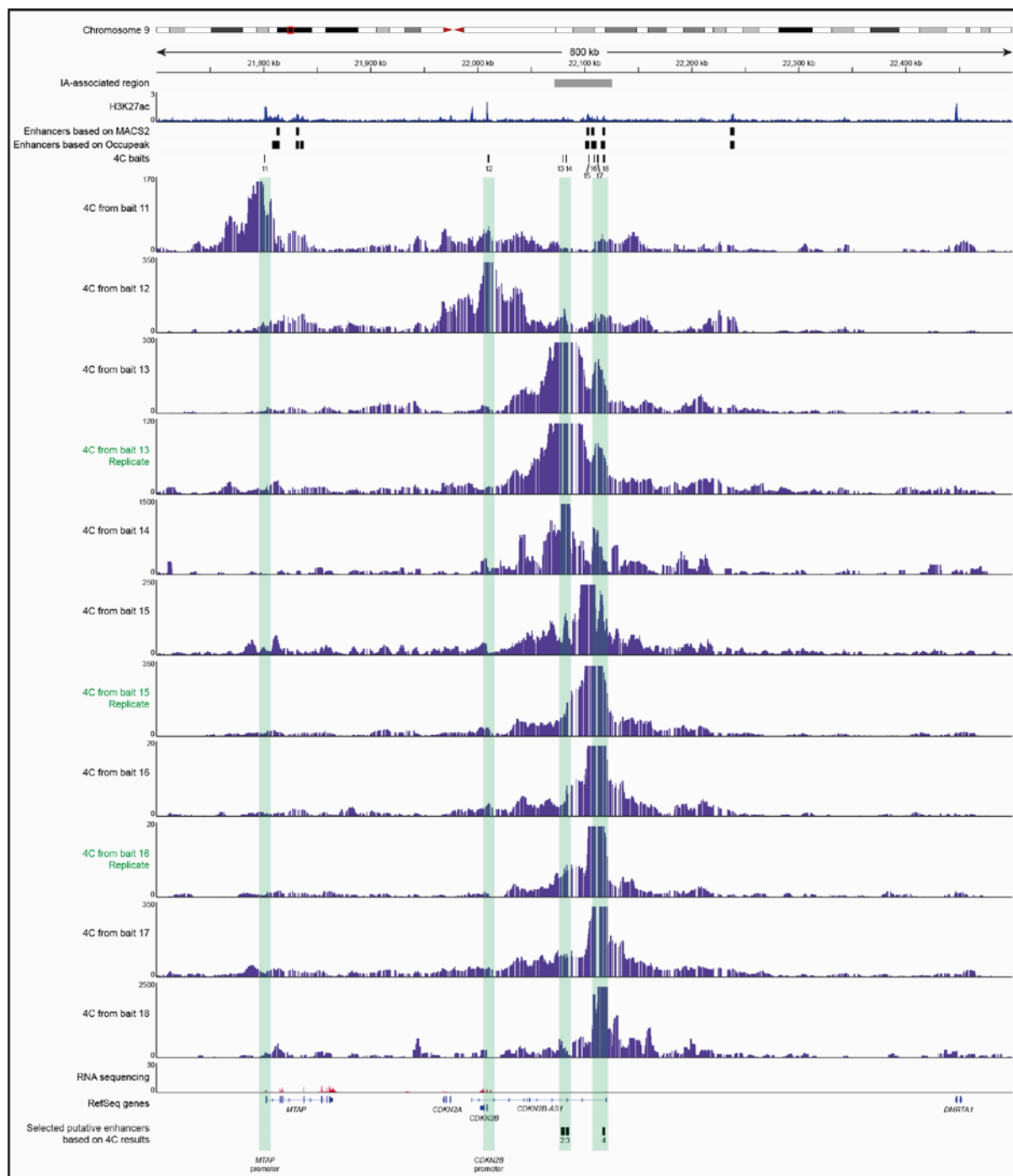
Genome browser view of a 1,100 kb example region on chromosome 4, that contains an IA-associated region. This graph shows a combination of multiple types of data. First, the localization of the IA-associated regions on the chromosome. Then, our previously published chromatin immunoprecipitation and sequencing (ChIP-seq) data for histone modification H3K27ac,[1] including the enhancer peaks called using peak calling algorithms MACS2[1] and Occupeak.[2] Next are the chromatin conformation capture (4C) baits that were selected by combining the results of the two peak calling algorithms. Then, the 4C results from this region for those of the 5 baits that were chosen for which the 4C experiment was successful, including a replicate (green). Baits 4 and 5 are promoters of the genes *EDNRA* and *TMEM184C*. Next are our previously published RNA sequencing data.[1] No putative enhancers were selected in this region since there was no evidence of interactions between enhancers and promoters.

Figure S4. Chromosomal interactions around the intracranial aneurysm (IA)-associated region on chromosome 8, including replicates.
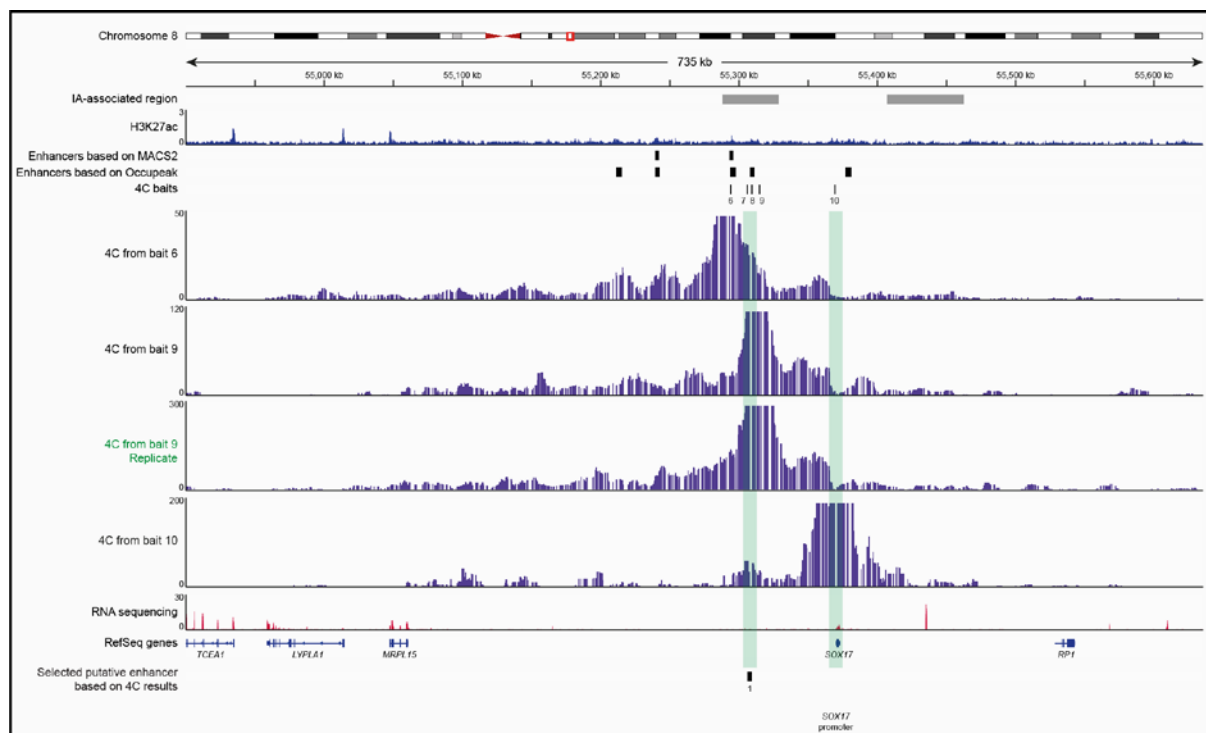
Genome browser view of a 735 kb example region on chromosome 8, that contains an IA-associated region. This graph shows a combination of multiple types of data. First, the localization of the IA-associated region on the chromosome. Then, our previously published chromatin immunoprecipitation and sequencing (ChIP-seq) data for histone modification H3K27ac,[1] including the enhancer peaks called using peak calling algorithms MACS2[1] and Occupeak.[2] Next are the chromatin conformation capture (4C) baits that were selected by combining the results of the two peak calling algorithms. Then, the 4C results from this region for those of the 5 baits that were chosen for which the 4C experiment was successful, including replicates (green). Baits 10 is the promoter of the gene *SOX17*. Next are our previously published RNA sequencing data.[1] Lastly, the graph shows the putative enhancer that was selected in this region, because of its interaction with the promoter of *SOX17*.

Figure S5. Chromosomal interactions around the intracranial aneurysm (IA)-associated region on chromosome 9, including replicates.

Genome browser view of a 800 kb example region on chromosome 9, that contains an IA-associated region. This graph shows a combination of multiple types of data. First, the localization of the IA-associated region on the chromosome. Then, our previously published

chromatin immunoprecipitation and sequencing (ChIP-seq) data for histone modification H3K27ac,[1] including the enhancer peaks called using peak calling algorithms MACS2[1] and Occupeak.[2] Next are the chromatin conformation capture (4C) baits that were selected by combining the results of the two peak calling algorithms. Then, the 4C results from this region for those of the 8 baits that were chosen for which the 4C experiment was successful, including replicates (green). Baits 11 and 12 are promoters of the genes *MTAP* and *CDKN2B* respectively. Next are our previously published RNA sequencing data.[1] Lastly, the graph shows the 3 putative enhancers that were selected in this region, because of their interaction with the promoters of *MTAP* and *CDKN2B*.

Figure S6. Chromosomal interactions around the intracranial aneurysm (IA)-associated region on chromosome 10, including replicates.
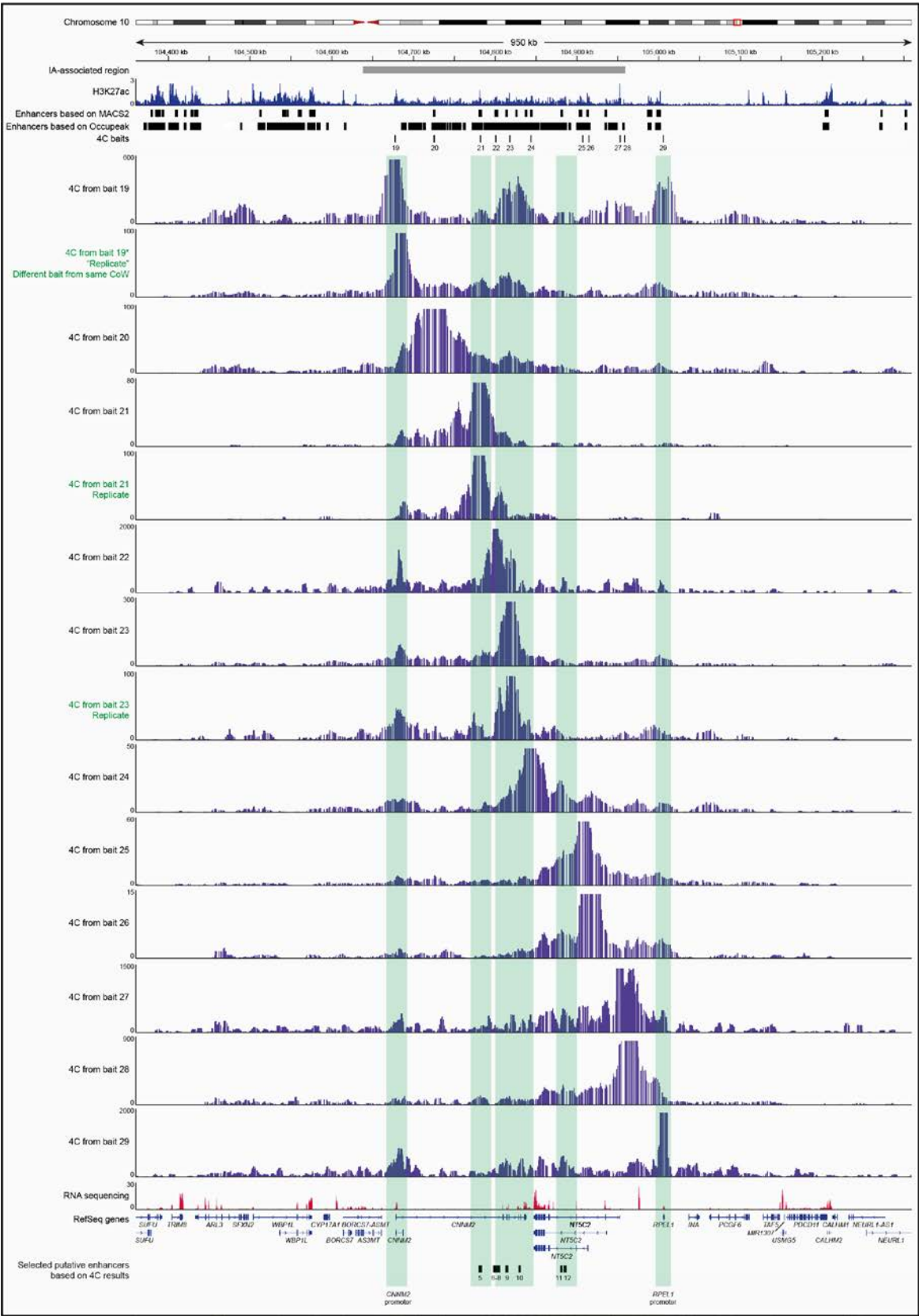
Genome browser view of a 950 kb example region on chromosome 10, that contains an IA-associated region. This graph shows a combination of multiple types of data. First, the localization of the IA-associated region on the chromosome. Then, our previously published chromatin immunoprecipitation and sequencing (ChIP-seq) data for histone modification H3K27ac,[1] including the enhancer peaks called using peak calling algorithms MACS2[1] and Occupeak.[2] Next are the chromatin conformation capture (4C) baits that were selected by combining the results of the two peak calling algorithms. Then, the 4C results from this region for those of the 11 baits that were chosen for which the 4C experiment was successful, including replicates (green). Baits 19 is the promoter of the gene *CNNM2*, baits 29 is the promoter of the gene *RPEL1*. Next are our previously published RNA sequencing data.[1] Lastly, the graph shows the 8 putative enhancers that were selected in this region, because of their interaction with the promoters of *CNNM2* and *RPEL1*.

**Figure S7. Selection of putative enhancers 6, 7, 8, 11 and 12.**
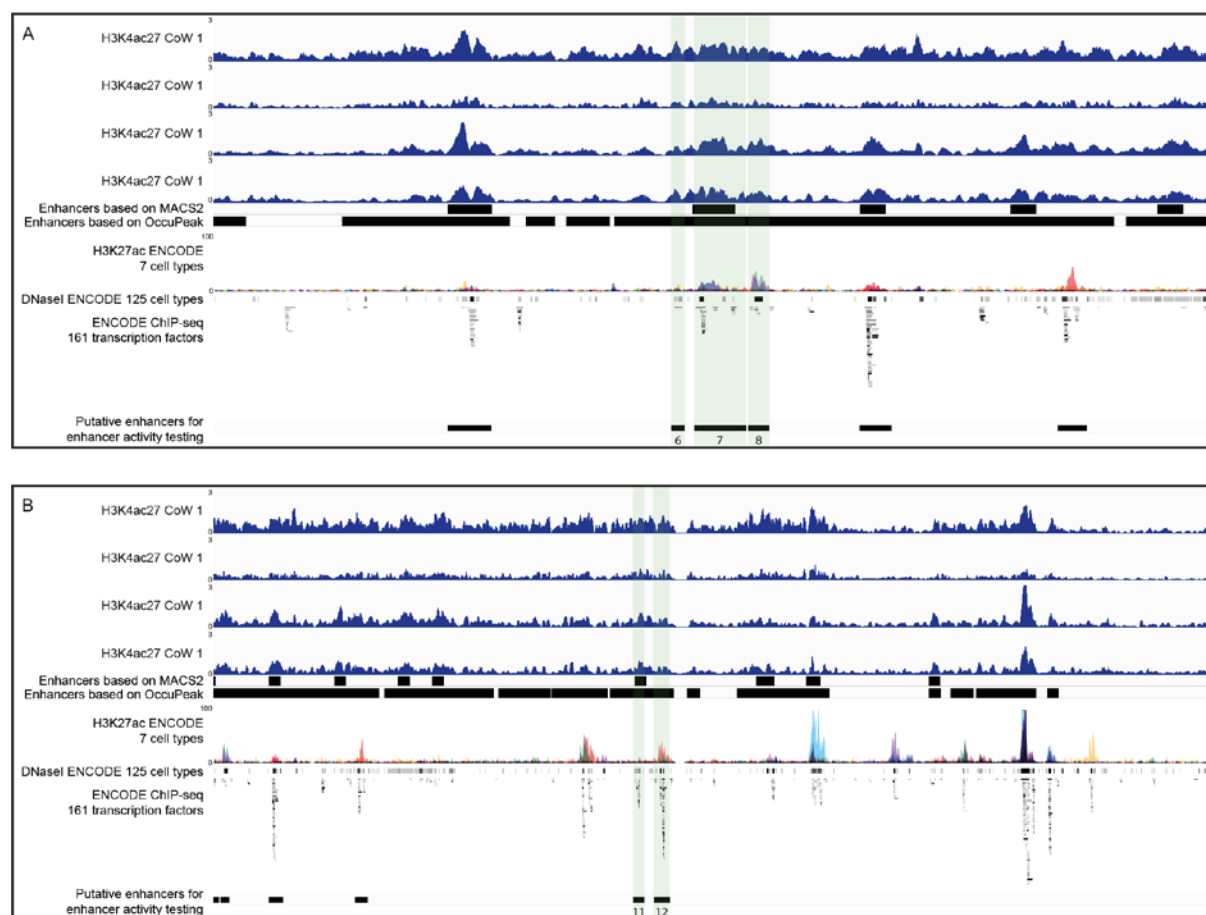
Two larger enhancer regions were divided into smaller individual putative enhancers (putative enhancers 6, 7 and 8 in panel A; putative enhancers 11 and 12 in panel B) based on H3K72ac chromatin immunoprecipitation and sequencing (ChIP-seq) results from 4 circles of Willis (CoWs)[1] (including the enrichment peaks called by the MACS21 and the OccuPeak2 algorithms), H3K27ac ChIP-seq from 7 cell types from ENCODE (derived from the UCSC genome browser), DNaseI hypersensitive clusters from 125 cell types from ENCODE (derived from the UCSC genome browser) and transcription factor ChIP-seq for 161 transcription factors from ENCODE (derived from the UCSC genome browser).

Figure S8. GFP fluorescence and brightfield images of injected zebrafish embryos between 3 and 4 days post fertilization (dpf).
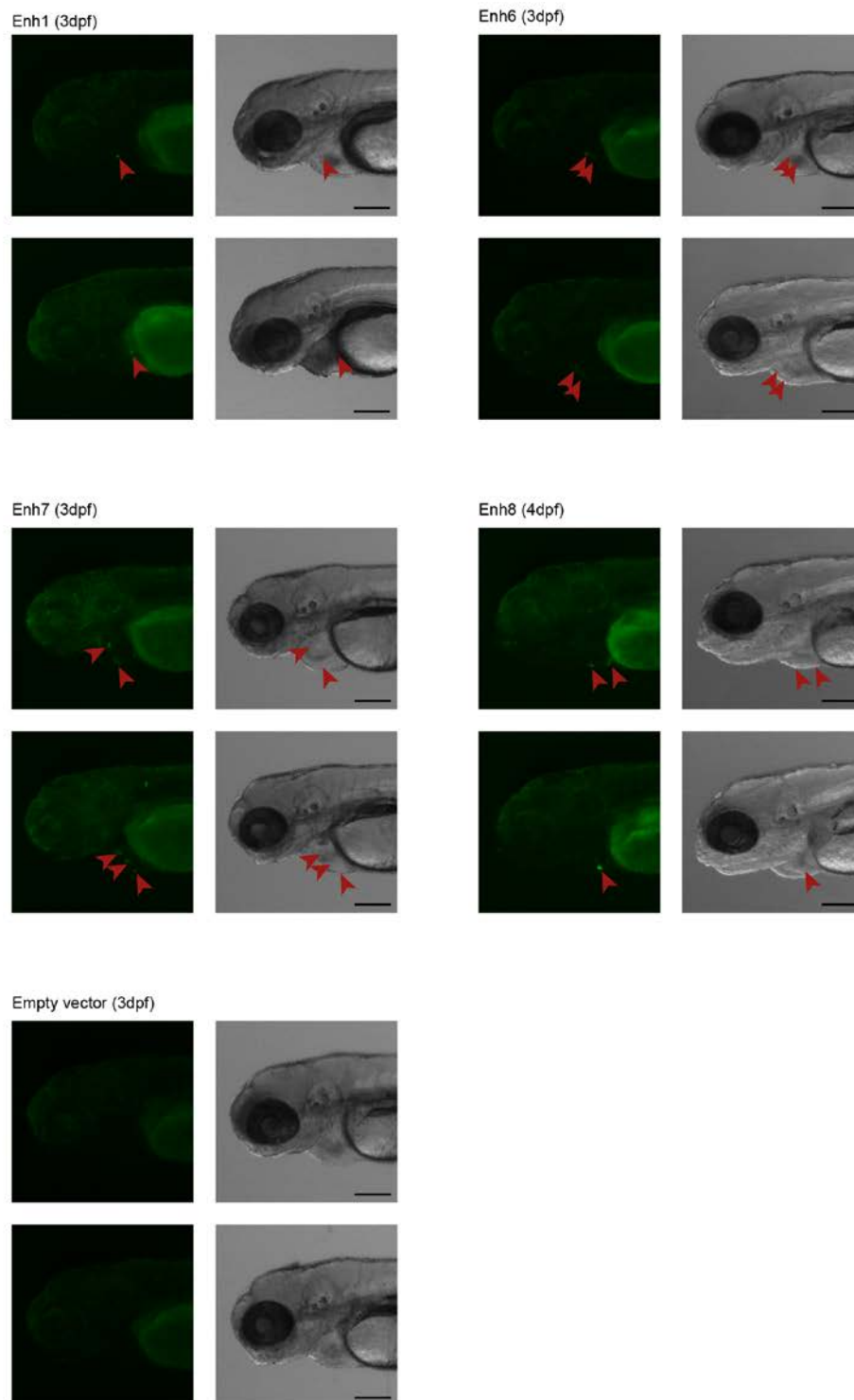
Enhancer activity results in clear green fluorescent protein (GFP) expression for Enh1 (heart; arrowheads), Enh6 (heart; arrowheads), Enh7 (heart; arrowheads) and Enh8 (heart; arrowheads), but no clear GFP expression was detected in embryos injected with the empty vector. Scale bars are 200µm.

Figure S9. Expression of control genes of interest in the circle of Willis (CoW).
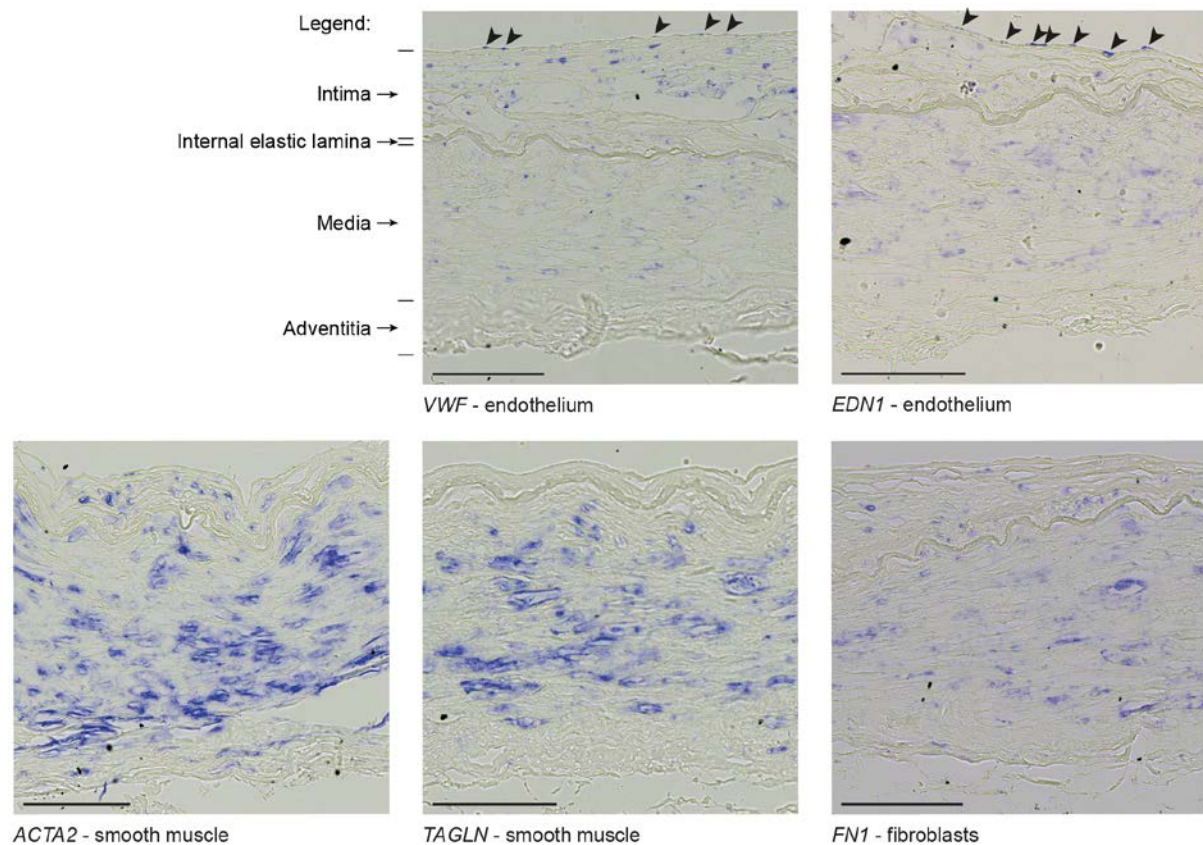
In situ hybridization (ISH) on CoW paraffin section shows the expression patterns of five genes in the CoW: *VWF* and *EDN1* (endothelium), *ACTA2* and *TAGLN* (smooth muscle) and *FN1* (fibroblasts). *VWF* and *EDN1* are the only genes that are expressed in endothelial cells (arrowheads) lining the lumen of the blood vessel. We have also detected (lower) expression in other cells throughout the intima and media of the CoW vessel wall for *VWF* and *EDN1*. *ACTA2* and *TAGLN* are strongly expressed in the media, where smooth muscle cells are mainly present. *ACTA2* is also expressed in the thickened intima, these cells are likely also smooth muscle cells that have infiltrated the intima. *FN1* is expressed throughout the thickened intima and media. Intima thickening likely results in other cells, such as smooth muscle cells and fibroblasts, infiltrating the intima3-7 in the microphotographs of *VWF*, *EDN1*, *ACTA2* and *FN1*. Scale bars are 100μm.

SUPPLEMENTAL REFERENCES:

1. Laarman MD, Vermunt MW, Kleinloog R, de Boer-Bergsma JJ, Brain Bank N, Rinkel GJE, et al. Intracranial Aneurysm–Associated Single-Nucleotide Polymorphisms Alter Regulatory DNA in the Human Circle of Willis. *Stroke*. 2018;49:447–453.

2. De Boer BA, Van Duijvenboden K, Van Den Boogaard M, Christoffels VM, Barnett P, Ruijter JM. OccuPeak: ChIP-seq peak calling based on internal background modelling. *PLoS One*. 2014;9:1–15.

3. Aziz M, Yadav KS. Pathogenesis of atherosclerosis. *Med. Clin. Rev.* 2016;2:1–6.

4. Ross R. The pathogenesis of atherosclerosis: a perspective for the 1990s. *Nature*. 1993;362:801–809.

5. Vukovic I, Arsenijevic N, Lackovic V, Todorovic V. The origin and differentiation potential of smooth muscle cells in coronary atherosclerosis. *Exp. Clin. Cardiol.* 2006;11:123–128.

6. Evrard SM, Lecce L, Michelis KC, Nomura-Kitabayashi A, Pandey G, Purushothaman KR, et al. Endothelial to mesenchymal transition is common in atherosclerotic lesions and is associated with plaque instability. *Nat. Commun.* 2016;7.

7. Wang D, Wang Z, Zhang L, Wang Y. Roles of Cells from the Arterial Vessel Wall in Atherosclerosis. *Mediators Inflamm.* 2017;2017.